

DICOM for quantitative imaging biomarker development: A standards based approach to sharing clinical data and structured PET/CT analysis results in head and neck cancer research

Andriy Fedorov, David Clunie, Ethan Ulrich, Christian Bauer, Andreas Wahle, Bartley Brown, Michael Onken, Jörg Riesmeier, Steve Pieper, Ron Kikinis, John Buatti, Reinhard R. Beichel

Background. Imaging biomarkers hold tremendous promise for precision medicine clinical applications. Development of such biomarkers relies heavily on image post-processing tools for automated image quantitation. Their deployment in the context of clinical research necessitates interoperability with the clinical systems. Comparison with the established outcomes and evaluation tasks motivate integration of the clinical and imaging data, and the use of standardized approaches to support annotation and sharing of the analysis results and semantics. We develop the methodology and tools to support these tasks in Positron Emission Tomography and Computed Tomography (PET/CT) quantitative imaging (QI) biomarker development applied to head and neck cancer (HNC) treatment response assessment, using the Digital Imaging and Communications in Medicine (DICOM®) international standard and free open source software.

Methods. Quantitative analysis of PET/CT imaging data collected on patients undergoing treatment for HNC was conducted. Processing steps included Standardized Uptake Value (SUV) normalization of the images, segmentation of the tumor using manual and semi-automatic approaches, automatic segmentation of the reference regions, and extraction of the volumetric segmentation-based measurements. Suitable components of the DICOM standard were identified to model the various types of data produced by the analysis. A developer toolkit of conversion routines and an Application Programming Interface (API) were contributed and applied to create a standards-based representation of the data.

Results. DICOM Real World Value Mapping, Segmentation and Structured Reporting objects were utilized for standards-compliant representation of the PET/CT QI analysis results and relevant clinical data. A number of correction proposals to the standard were developed. The open source DICOM toolkit (DCMTK) was improved to simplify the task of DICOM encoding by introducing new API abstractions. Conversion and visualization tools utilizing this toolkit were developed. The encoded objects were validated for consistency and interoperability. The resulting dataset was deposited in the QIN-HEADNECK collection of The Cancer Imaging Archive. Supporting tools for data analysis and DICOM conversion were made available as free open source software.

Discussion. We presented a detailed investigation of the development and application of the DICOM model, as well as the supporting open source tools and toolkits, to accommodate representation of the research data in QI biomarker development. We demonstrated that the DICOM standard can be used to represent the types of data relevant in HNC QI biomarker development, and encode their complex relationships. The resulting annotated objects are amenable to data mining applications, and are interoperable with a variety of systems that support the DICOM standard.

1 DICOM for quantitative imaging biomarker development: A
2 standards-based approach to sharing clinical data and
3 structured PET/CT analysis results in head and neck
4 cancer research

5 *Andriy Fedorov*^{1,2}, *David Clunie*³, *Ethan Ulrich*⁴, *Christian Bauer*^{4,5}, *Andreas Wahle*^{4,5},
6 *Bartley Brown*⁶, *Michael Onken*⁷, *Jörg Riesmeier*⁸, *Steve Pieper*⁹, *Ron Kikinis*^{1,2,10,11},
7 *John Buatti*¹², *Reinhard R. Beiche*^{4,5,13}

8 ¹ Department of Radiology, Brigham and Women's Hospital, Boston, Massachusetts, United States of
9 America

10 ² Harvard Medical School, Harvard University, Boston, Massachusetts, United States of America

11 ³ PixelMed Publishing, LLC, Bangor, Pennsylvania, United States of America

12 ⁴ Department of Electrical and Computer Engineering, University of Iowa, Iowa City, Iowa, United States
13 of America

14 ⁵ Iowa Institute for Biomedical Imaging, University of Iowa, Iowa City, Iowa, United States of America

15 ⁶ Center for Bioinformatics and Computational Biology, University of Iowa, Iowa City, Iowa, United States
16 of America

17 ⁷ Open Connections GmbH, Oldenburg, Germany

18 ⁸ Freelancer, Oldenburg, Germany

19 ⁹ Isomics, Inc., Cambridge, Massachusetts, United States of America

20 ¹⁰ Fraunhofer MEVIS, Bremen, Germany

21 ¹¹ Mathematics/Computer Science Faculty, University of Bremen, Germany

22 ¹² Department of Radiation Oncology, University of Iowa Carver College of Medicine, Iowa City, Iowa,
23 United States of America

24 ¹³ Department of Internal Medicine, University of Iowa, Iowa City, Iowa, United States of America
25

26 Corresponding author: *Andriy Fedorov*^{1,2}

27 1249 Boylston St #344, Boston, MA 02215, USA

28 email: andrey.fedorov@gmail.com or fedorov@bwh.harvard.edu.

29

30

31

32 **Abstract**

33 **Background.** *Imaging biomarkers hold tremendous promise for precision medicine clinical*
34 *applications. Development of such biomarkers relies heavily on image post-processing tools for*
35 *automated image quantitation. Their deployment in the context of clinical research necessitates*
36 *interoperability with the clinical systems. Comparison with the established outcomes and*
37 *evaluation tasks motivate integration of the clinical and imaging data, and the use of*
38 *standardized approaches to support annotation and sharing of the analysis results and*
39 *semantics. We develop the methodology and tools to support these tasks in Positron Emission*
40 *Tomography and Computed Tomography (PET/CT) quantitative imaging (QI) biomarker*
41 *development applied to head and neck cancer (HNC) treatment response assessment, using*
42 *the Digital Imaging and Communications in Medicine (DICOM®) international standard and free*
43 *open source software.*

44 **Methods.** *Quantitative analysis of PET/CT imaging data collected on patients undergoing*
45 *treatment for HNC was conducted. Processing steps included Standardized Uptake Value*
46 *(SUV) normalization of the images, segmentation of the tumor using manual and semi-*
47 *automatic approaches, automatic segmentation of the reference regions, and extraction of the*
48 *volumetric segmentation-based measurements. Suitable components of the DICOM standard*
49 *were identified to model the various types of data produced by the analysis. A developer toolkit*
50 *of conversion routines and an Application Programming Interface (API) were contributed and*
51 *applied to create a standards-based representation of the data.*

52 **Results.** *DICOM Real World Value Mapping, Segmentation and Structured Reporting objects*
53 *were utilized for standards-compliant representation of the PET/CT QI analysis results and*
54 *relevant clinical data. A number of correction proposals to the standard were developed. The*
55 *open source DICOM toolkit (DCMTK) was improved to simplify the task of DICOM encoding by*
56 *introducing new API abstractions. Conversion and visualization tools utilizing this toolkit were*
57 *developed. The encoded objects were validated for consistency and interoperability. The*
58 *resulting dataset was deposited in the QIN-HEADNECK collection of The Cancer Imaging*
59 *Archive. Supporting tools for data analysis and DICOM conversion were made available as free*
60 *open source software.*

61 **Discussion.** *We presented a detailed investigation of the development and application of the*
62 *DICOM model, as well as the supporting open source tools and toolkits, to accommodate*
63 *representation of the research data in QI biomarker development. We demonstrated that the*
64 *DICOM standard can be used to represent the types of data relevant in HNC QI biomarker*
65 *development, and encode their complex relationships. The resulting annotated objects are*
66 *amenable to data mining applications, and are interoperable with a variety of systems that*
67 *support the DICOM standard.*

68

69

70

71

72 Introduction

73 Imaging has enormous untapped potential to improve clinical cancer treatment decision making.
74 To harness this potential, research exploring the utility of image analysis to extract and process
75 morphometric and functional biomarkers is essential. In the era of non-cytotoxic treatment
76 agents, multi-modality image-guided therapies and rapidly evolving computational resources,
77 quantitative imaging software performing such analyses can be transformative for precision
78 medicine by enabling minimally invasive, objective and reproducible evaluation of image-based
79 cancer treatment targeting and response. Post-processing algorithms are integral to high-
80 throughput analysis and fine-grained differentiation of multiple molecular targets. Software tools
81 used for such analyses must be robust and validated across a range of datasets collected for
82 multiple subjects, acquisition devices, timepoints and institutions. Ensuring the validity of this
83 software requires unambiguous specification of analysis protocols, documentation of the
84 analysis results, and clear guidelines for their interpretation. Yet cancer research imaging data
85 often does not exist in consistent formats that facilitate advancement of quantitative analysis.
86 The infrastructure to support common data exchange and method sharing is lacking. These
87 issues hinder development, validation and comparison of new approaches, secondary analysis
88 and discovery of data, and comparison of results across sites and methodologies.

89 Recent initiatives such as the Quantitative Imaging Network (QIN) and Informatics Technology
90 for Cancer Research (ITCR) of the National Cancer Institute (NCI), and Quantitative Imaging
91 Biomarker Alliance (QIBA) of the Radiological Society of North America (RSNA) focus on a
92 spectrum of issues related to quantitative imaging (QI) biomarker development, including both
93 the validation and deployment of promising QI tools, and the development of the supporting
94 infrastructure. Quantitative Image Informatics for Cancer Research (QIICR) is one of the
95 projects of the ITCR consortium (<http://qiicr.org>, U01 CA190819). The overarching mission of
96 QIICR is to provide Free and Open Source Software (FOSS) QI analysis tools accompanied by
97 the imaging data and analysis results stored in a standards-compliant structured fashion to
98 support imaging biomarker development. Ultimately, our goal is to facilitate both the reuse of the
99 shared research data and the acceleration of the translation of the QI methods and tools into
100 clinical practice. QIICR is a collaboration with three sites of the NCI QIN (namely, Brigham and
101 Women's Hospital, University of Iowa, and Massachusetts General Hospital), each of which is
102 focused on different diseases, and uses different imaging technologies and analysis methods.
103 The research projects of interest at these three sites serve as use cases and testbeds for
104 driving the requirements, testing and dissemination of the imaging informatics technology being
105 developed by QIICR.

106 In this paper, we focus on one of the QIICR use cases — PET/CT QI biomarker development
107 for treatment response in head and neck cancer (HNC) — to demonstrate how the use of the

108 Digital Imaging and Communications in Medicine (DICOM^{®1}) international standard (National
109 Electrical Manufacturers Association (NEMA)), in conjunction with FOSS tools, can enable
110 interoperable sharing of the quantitative imaging analysis results. The contributions of this work
111 are twofold. First, we propose a DICOM-based approach to data sharing in QI research, and
112 present the resulting dataset of clinical information and analysis results generated by a clinical
113 research study investigating QI biomarkers in Positron Emission Tomography and Computed
114 Tomography (PET/CT) imaging for predicting therapy outcome in the patients undergoing
115 treatment for HNC. Second, we develop a suite of FOSS tools to facilitate encoding of the
116 analysis results using the DICOM standard.

117 The research study that generated the data described in this work investigated the use of
118 quantitation of the [18F]-fluorodeoxyglucose (FDG) tracer uptake in PET/CT images (CT is
119 combined with PET for attenuation compensation as well as spatial localization). FDG PET/CT
120 is commonly used for localization, characterization and qualitative assessment of therapy
121 response in a variety of malignancies (Larson et al., 1999; Weber, 2006). Quantitative
122 assessment of tumor burden using FDG PET/CT relies on a number of analysis steps, and can
123 be sensitive to the processing technique and definition of the volumetric Region of Interest (ROI)
124 (Boellaard, 2009; Vanderhoek, Perlman & Jeraj, 2012). A goal of the study that generated the
125 data was to investigate the process of PET quantitation and propose improved ROI
126 segmentation tools and a reproducible PET/CT quantitative analysis workflow. Steps involved in
127 the analysis of the PET/CT images included normalization of the PET image data using the
128 Standardized Uptake Value (SUV) body weight factor, segmentation of the tumor and involved
129 lymph nodes using both manual and automated segmentation tools, and quantitation of various
130 statistics related to the tracer uptake from the segmented ROIs. The processing steps and their
131 interactions are shown in Fig. 1, and are detailed in the Methods section.

132 Most of the methods used for QI analysis that produced the data presented in this paper are
133 accompanied by FOSS tools developed as part of the QIICR project. However, the main
134 objective of this paper is not to discuss these analysis methods in detail, or to validate the tools
135 implementing those analysis methods. Instead, we focus on the use of DICOM to enable
136 structured, standardized, and interoperable communication of the annotated analysis results
137 produced by those tools. Our goal is to facilitate access to the data and analysis results so other
138 research groups can perform similar validation, compare the results to different methods or
139 apply new tools to the imaging data.

140 Interoperability can be defined as “a property of a product or system, whose interfaces are
141 completely understood, to work with other products or systems, present or future, without any
142 restricted access or implementation” (Interoperability Working Group (AFUL), 2015).
143 Interoperability implies the use of a common standard — ideally, an open standard — to engage
144 the broad community of various stakeholders in industry and academia. We chose DICOM as
145 the common standard, due to its broad and inclusive community of contributors, its ubiquitous
146 adoption in the medical imaging domain and the suitability of its data model to accommodate
147 the requirements of the use case. For rapidly evolving research applications like imaging

¹ DICOM is the registered trademark of the National Electrical Manufacturers Association (NEMA) for its standards publications relating to digital communications of medical information.

148 biomarker development, it is also important to note that DICOM is a standard that is being
149 continuously refined to address new community demands and technologies, while maintaining
150 backwards compatibility with the existing user base. This process is enabled via the mechanism
151 of Correction Proposals (CPs) and Supplements that can be submitted for consideration and
152 review by the DICOM community, and are integrated into the standard through the formal
153 process of discussion, refinement and voting.

154 DICOM is primarily used to support interoperability between clinical systems for image
155 interchange (Haak et al., 2015). Consumption of the DICOM images produced by preclinical and
156 clinical acquisition systems is widely supported in research tools, making an ever-growing
157 stream of imaging data available to researchers. Sharing of results between different groups is
158 widely regarded as a priority (Stodden, 2010; Walport & Brest, 2011; Boulton et al., 2011;
159 Piwowar & Vision, 2013) and the failure to adopt standards for encoding results is flagged as a
160 critical barrier (Chan et al., 2014). We argue (and demonstrate by example in this paper) that
161 DICOM provides the means to support interchange of not only acquired images but also clinical
162 data and various types of analysis results, with the goal of enabling their sharing and reuse. We
163 recognize that the output of analysis results using DICOM is severely limited or non-existent in
164 current tools. Instead, research tools often default to using locally defined or domain-specific
165 formats (Kindlmann, 2004; Ibanez & Schroeder, 2005; Schroeder & Martin, 2005; NifTI Data
166 Format Working Group, 2005; MRC Cognition and Brain Sciences Unit, 2013), while
167 commercial tools often limit export of the analysis results or utilize proprietary mechanisms. The
168 research formats cover narrow use cases in restricted domains, ultimately compromising
169 consistency, dissemination and reuse of the analysis results by fellow researchers. One of our
170 objectives is to remedy this situation and provide the missing support of DICOM for QI
171 applications in tools and toolkits.

172 Interoperable communication of analysis results between research and clinical systems is
173 another critical consideration for validation and translation of QI precision medicine tools. The
174 development and evaluation of research applications, data and software historically proceeds
175 independently from clinical care and in distinct systems. Yet the extent to which data and
176 software are interoperable between research and clinical environments directly impacts the
177 ability to use clinical data for research, to use research applications in experimental clinical care,
178 and to then translate research developments into clinical practice. Many barriers to such
179 “translational” scenarios have been identified, among them being failure to use standard models
180 and encoding formats in research and clinical environments (Katzan & Rudick, 2012; Chan et
181 al., 2014) and failure to use standard codes (McDonald, Vreeman & Abhyankar, 2013).

182 Recent publications demonstrate that there is an increased recognition of the value of at least
183 exporting images that are the result of research processing applications in DICOM format, so
184 that they can be used to support various activities essential for imaging biomarker development
185 (Krishnaraj et al., 2014). Such activities include consistently “tagging” analysis results to
186 compare analyses done at different centers on different cohorts using different analysis tools
187 (Waterton & Pylkkanen, 2012), supporting archival and distribution of the analysis results in a
188 manner that enables indexing and secondary analysis (Chan et al., 2014) and transfer to and
189 visualization of the analysis results in clinical systems in which metadata for patient identification
190 and study management is required (Clark et al., 2013; Moore et al., 2015).

191 DICOM relies on coded terminology (Bidgood, 1997), both from standard external lexicons
192 (such as the Systematized Nomenclature of Medicine (SNOMED^{®2}) (Bidgood, 1998) as well as
193 from the DICOM lexicon (National Electrical Manufacturers Association (NEMA), 2016a) when
194 no suitable external terms are available (Bidgood et al., 1997). The “semantic” approach of
195 using standard codes allows for greater reuse and harmonization with other data sets, since the
196 need for natural language parsing of plain text during “data mining” is obviated by the
197 commonality of standard codes for standard entities, such as anatomical regions, types of
198 tumor, etc. (in the same manner as the “semantic web” (“Semantic Web - W3C,” 2015)).

199 The arguments presented above for the benefits of open standards such as DICOM are widely
200 accepted, however adoption of such standards is not without effort. The DICOM standard is
201 widely and fairly regarded in the research community as being non-trivial in complexity, while its
202 documentation is extensive and difficult to navigate. Support of DICOM in toolkits is widespread,
203 but mostly limited to the lower-level abstractions and more commonly oriented towards
204 consuming rather than producing DICOM objects³. Reference implementations and sample
205 datasets illustrating the application of the certain parts of the standard are often absent. As with
206 any complex endeavor, the DICOM standard itself is not without errors and may contain internal
207 contradictions. The standard does not have (and does not claim to have) all of the features that
208 are needed to support new or uncommon research use cases. These are some of the real
209 obstacles for adoption of DICOM for communicating analysis results, both among
210 manufacturers of commercial imaging workstations and within the QI research community.

211 In this contribution we take a number of steps to rectify this situation. We demonstrate the
212 application of the DICOM standard to model and share a real example of a complex research
213 dataset. We accompany this demonstration with the resulting dataset, source code of the
214 conversion tools we used, developer toolkit and Application Program Interface (API) that we
215 used to develop the conversion tools, and integrated user-level analysis and visualization tools,
216 all available as FOSS. We provide detailed explanation of, and motivation for, using specific
217 parts of the standard. Finally, we demonstrate how the standard itself can be improved via the
218 community review process, to address errors and limitations, which can best be identified and
219 solved by applying the standard to a real use case.

220 Materials and Methods

221 *Patient cohort selection*

222 The primary data was extracted from HNC patients with squamous cell carcinoma, all treated
223 according to the standard of care at the University of Iowa Hospital and Clinics. Clinical practice
224 was to obtain a FDG PET/CT for staging (prior to treatment) and then a second FDG PET/CT
225 scan for response assessment at approximately three months following the completion of the
226 initial therapy. All patient data was collected in compliance with HIPAA regulations under
227 approval granted by the internal review board of the University of Iowa, approval #200503706.

² SNOMED is a registered trademark of the International Health Terminology Standards Development Organisation (IHTSDO).

³ The colloquial term “object” is used throughout this paper for clarity, rather than “instance”, “class”, or the more formal terms used in the DICOM standard, Information Object Definition (IOD) or Service-Object Pair Class (SOP Class).

228 Written consent was obtained from the study participants. The imaging studies were acquired
229 between 2004 and 2013. Patients that had a baseline and at least one post-therapy follow-up
230 PET/CT were included in the research study. Patients were followed clinically and outcomes
231 were available with a minimum of 2 years of follow-up. Patients may have had additional
232 imaging studies following the three month response assessment FDG PET/CT based on clinical
233 judgment and findings.

234 Clinical metadata for each patient was manually extracted from the electronic health records
235 and included sex, age, smoking, and drinking history as well as pathology, stage, primary site
236 location, and detailed location of involved nodal sites. Treatment details (e.g., radiation dose,
237 technique, surgical intervention and chemotherapy delivery) and disease status and recurrences
238 were recorded. All clinical metadata was de-identified and stored in a Postgres relational
239 database locally. Measurements made on images that were used for clinical purposes and
240 stored in the clinical records were not used during the conversion process, since new
241 measurements were to be made, and homogeneity and accuracy of the clinical measurements
242 could not be easily verified.

243 A total of 156 patients were identified as eligible for the study, with at least one PET/CT scan
244 and related clinical data available for study (mean 3.05 studies/patient collected during a total of
245 472 visits). Fifty-nine patients from the cohort were processed using the methodology described
246 in the following text. In one of those 59 patients both pre- and post-treatment imaging studies
247 were processed, while in the rest of the patients only the baseline scan was analyzed.

248 *Image acquisition*

249 Pertinent details related to image acquisition such as reconstruction procedure, image
250 resolution and injected dose were encoded in the DICOM image metadata by the scanner. After
251 initial de-identification, the image data was stored in an eXtensible Neuroimaging Archive
252 Toolkit (XNAT) (Marcus et al., 2007) local research archive at the University of Iowa.

253 *Image processing*

254 SUV is commonly utilized for a simple semi-quantitative analysis of PET images (Lucignani,
255 Paganelli & Bombardieri, 2004). SUV Body Weight (SUVbw) is defined as the ratio of activity in
256 tissue divided by the decay-corrected activity injected to the patient, normalized by body weight:
257 $SUVbw = (\text{tissue activity}) / (\text{injected activity} / \text{weight})$. Several alternatives to SUVbw approach
258 have been investigated including body surface area corrected (SUVbsa) and lean body mass
259 corrected (SUVlbm) (Graham, Peterson & Hayward, 2000), but SUVbw remains the most
260 commonly utilized quantity.

261 There are several underlying assumptions made in using FDG SUVs for measuring metabolic
262 activity in lesions, such as accurate measurement of injected dose and accurate decay
263 correction of all measurements (Graham, Peterson & Hayward, 2000). The failure of one or
264 more of these assumptions can introduce variability in calculated SUVs. To mitigate this
265 problem, an SUV ratio (SUVr) can be used, which represents the ratio of the SUV of a lesion to
266 the SUV of a normal tissue Reference Region (RR) defined in the same acquisition.

267 In the project generating the data presented here, the primary cancer site and all involved lymph
268 nodes were segmented separately to allow quantification of SUV for either the primary cancer
269 site alone, total tumor burden, or on a per-region basis. Segmentation of the primary tumor and

270 lymph nodes was done using two interactive segmentation tools within 3D Slicer (Fedorov et al.,
271 2012). The first tool is a manual contouring tool, requiring the user to draw the boundary of a
272 lesion on every slice using the Editor module of 3D Slicer. The second tool is semi-automated,
273 performing segmentation in 3D using a specialized algorithm for segmenting HNC in FDG PET
274 images, which is described and evaluated in detail in (Van Tol et al., 2016). This semi-
275 automated segmentation approach treats the segmentation task as a graph-based optimization
276 problem based on the ideas introduced by Yin et al. (Yin et al., 2010). Starting with a user-
277 provided approximate lesion center point, a graph structure is constructed in a local
278 neighborhood, and a suitable cost function is derived based on local image statistics. A
279 maximum flow algorithm is used for optimization. The resulting segmentation is converted from a
280 graph-based representation to a labeled volume. To handle frequently occurring situations that
281 are ambiguous, several segmentation modes are introduced to adapt the behavior of the base
282 algorithm accordingly. In addition, “just enough interaction” based approaches are provided to
283 enable the user to efficiently perform local and/or global refinement of initial segmentations. This
284 semi-automated segmentation method is implemented in the PET Tumor Segmentation
285 extension of 3D Slicer (QIICR, 2015a).

286 Since both manual and semi-automatic methods for HNC segmentation depend on user input,
287 results are expected to be subject to intra- and inter-operator variation. To allow assessment of
288 the impact of such variation on subsequent processing steps, each data set was reviewed and
289 segmented using both methods by three readers, who were experts in HNC PET/CT image
290 interpretation. Images were presented to the readers in random order. For each combination of
291 the segmentation tool and reader, this process was performed twice, resulting in twelve
292 segmentation sessions per patient. RRs in liver, cerebellum, and aortic arch were segmented
293 automatically using the approach we presented earlier (Bauer et al., 2012).

294 Given the segmentations of the primary tumor and lymph nodes, a total of 22 quantitative
295 indices were extracted from each of these regions using the *PET-IndiC* extension of 3D Slicer
296 (QIICR, 2015b). The calculated quantitative indices consist of commonly utilized PET-specific
297 indices such as maximum, mean and peak SUV (Wahl et al., 2009) and Total Lesion Glycolysis
298 (TLG), as well as common summary statistics, which included median, variance and Root Mean
299 Square (RMS) of SUV, and segmentation volume. Mean, maximum, minimum, standard
300 deviation, median, and first and third quartiles were calculated for RRs.

301 *Data modeling and conversion into DICOM representation*

302 The DICOM standard provides a variety of objects that can be used to communicate information
303 derived from the images. Regardless of the specific object type, DICOM requires that all objects
304 contain so-called “composite context”. At the patient level, the composite context includes
305 identifying and descriptive attributes such as patient name, ID, age and sex. The study context
306 includes the date and time that the imaging study started, unique identification of the study and
307 other information common to all series in the study. The composite context enables consistent
308 indexing and cross-referencing of the various objects. In addition to shared composite context,
309 derived DICOM objects typically contain explicit references to the “source” objects from which
310 they were derived, which supports recording of the provenance of the object derivation as well
311 as application functionality such as superimposition during rendering. Various relationships
312 between the objects used in this study are shown in Fig. 2.

313 In the following sections we discuss the motivation for the choice of specific DICOM objects. We
314 start with the PET and CT objects, since they were produced by the acquisition equipment and
315 underwent only minor editing for de-identification. Next we describe the objects containing
316 patient clinical data (clinical history and outcomes). Then we cover the derived imaging objects
317 from simple to more complex:

- 318 • DICOM Real-World Value Mapping (RWVM) objects encode mapping of the image-
319 specific SUV factor that is needed for normalization of the images and subsequent
320 processing;
- 321 • DICOM Segmentation (SEG) objects encode labeling of the PET and CT image voxels
322 into anatomical structures, such as primary tumor and liver ROI;
- 323 • DICOM Structured Reporting (SR) objects encode various measurements computed
324 from the segmentation-defined regions on the normalized PET image volumes.

325 We follow the general pattern of discussing the scope and capabilities of the object at a high
326 level, followed by an abbreviated summary of the design decisions made to meet the
327 requirements of our use case. The reader is referred to the preprint version of this article
328 (Fedorov et al., 2015a) for further discussions, which has been omitted for brevity. Corrections
329 to DICOM that resulted directly from our experience are also listed. A separate section covers
330 the implementation details of converting research representations into the DICOM format, and
331 references the tools we developed for this purpose.

332 *PET/CT Image Data*

333 PET and CT image data were stored in the DICOM Positron Emission Tomography Image
334 (National Electrical Manufacturers Association (NEMA), 2016b) and Computed Tomography
335 Image (National Electrical Manufacturers Association (NEMA), 2016c), respectively. The image
336 data obtained from the scanner was de-identified using a modified version of the Basic Attribute
337 Confidentiality Profile defined by the DICOM in PS3.15 Appendix E.2 (National Electrical
338 Manufacturers Association (NEMA), 2016d). Image de-identification was performed following
339 the standard operational procedures established by The Cancer Imaging Archive (TCIA) (Clark
340 et al., 2013; Moore et al., 2015). Research identifiers of the form QIN-HEADNECK-01-nnnn
341 were assigned in place of the patient names and medical record numbers. Dates were shifted
342 by the same fixed offset across all the datasets to maintain temporal relationships of the
343 datasets. The de-identified images were then used for the remainder of the project (i.e., to make
344 the measurements and convert them into derived DICOM objects), in order to mitigate the risk
345 of leakage of patient identifiers into the publicly accessible analysis results.

346 *Clinical Information: DICOM SR*

347 Relevant clinical information available for the subjects enrolled in the study included clinical
348 history (such as the diagnosis and pathology, surgery and radiotherapy administration, and
349 demographics) and outcomes (follow-up date and status, and the date of death, when
350 applicable). This information is important for the interpretation and secondary reuse of the
351 image and quantitative data set, since it contains the clinically relevant end-points for the
352 evaluation of the biomarker performance, and it provides non-imaging predictors that can be
353 used for machine learning. The clinical information was extracted from the operational Postgres

354 research database, and retrospectively encoded in DICOM SR, one SR object per patient. The
355 choice of DICOM SR for encoding clinical information is explained in Appendix 1.

356

357 DICOM SR objects (sometimes referred to as SR “documents”) contain information organized
358 as a hierarchical content “tree” consisting of content items (tree nodes) (Clunie, 2000). These
359 content items include containers, textual information, codes describing concept names (we will
360 use “term” and “concept” interchangeably in this document) and values (where appropriate),
361 references to images, and numeric values (National Electrical Manufacturers Association
362 (NEMA), 2016e). DICOM SR templates define a pattern of content items and their relationships,
363 constraining the general infrastructure for specific use cases (National Electrical Manufacturers
364 Association (NEMA), 2016f). Each SR template is assigned a Template Identifier (TID).
365 Templates may define the entire content of an object (i.e., be a “root” template) or may be a
366 reusable common pattern of nested content to be included by higher level templates (i.e., be a
367 “subordinate” template).

368 Each content item, except for those that are containers, can be thought of as a “name-value
369 pair” (or alternatively, as a “question” and an “answer”). Containers can be considered “section
370 headings”, and are often explicitly used as such when rendered in human-readable form. The
371 top level (root node) of the content tree is always a container, and its name (concept) is often
372 referred to as the “document title”. The concept name of a container or name-value pair
373 (mandatory in most cases) is always coded using a code from a controlled terminology. The
374 value may or may not be coded depending on the value type.

375 The use of controlled terminology is fundamental to DICOM SR. DICOM SR codes are defined
376 as triplets of code value, coding scheme designator and code meaning (e.g., (F-02573, SRT,
377 “Alcohol consumption”), where “SRT” is the DICOM designation for the SNOMED coding
378 scheme). While DICOM allows for reuse of the codes defined in other terminologies, such as
379 SNOMED, as well as those defined in the DICOM standard itself, so called “private” codes can
380 also be defined by the creator of the object, when no standard codes are available. Such private
381 codes are distinguished by a coding scheme designator that starts with a “99” prefix. The use of
382 predefined codes not only provides semantic information, but also simplifies validation of the
383 resulting objects. The codes that are allowed are constrained by the template. The constraints
384 for values may be defined in the template itself, or in a “value set”, which in DICOM is called a
385 Context Group (and labeled with a Context Group ID (CID)).

386 Though DICOM contains templates for clinical data for a few specific applications (e.g.,
387 cardiovascular (National Electrical Manufacturers Association (NEMA), 2016g) and breast
388 (National Electrical Manufacturers Association (NEMA), 2016h)), it does not define a template to
389 represent all the clinical data items of interest in our HNC QI research use case. Given the lack
390 of a suitable standard template to represent this data, we developed our own set of custom
391 templates for communicating the clinical information. In DICOM, such custom templates are
392 referred to as “private templates”, even though they may be publicly shared and are required to
393 be documented in the DICOM conformance statement of the product. These templates included
394 information about biopsy, treatment and other relevant data. The relationships between the
395 private templates are shown in Fig.3, with a detailed description provided in Appendix 2. These

396 templates follow the patterns of existing DICOM templates, with the intent that they might form
397 the basis for future enhancements of the standard.

398 No structured terminology was used at the time of initial clinical data collection, so terms with
399 codes were selected retrospectively at the time of conversion of the data to DICOM SR. Our
400 approach for selecting codes leveraged SNOMED (Cornet & de Keizer, 2008) and UMLS
401 (Bodenreider, 2004) terminology as much as possible. The few concepts that could not be
402 located in the SNOMED, UMLS or DICOM terminologies were added to a private coding
403 scheme. All of the codes that are of relevance to this project are listed in Appendix 2.

404 *Standardized Uptake Value: DICOM RWVM*

405 The DICOM Real World Value Mapping (RWVM) object provides a mechanism to describe the
406 calculation that was used (and can be reused) to create “real world values” (such as SUV) from
407 stored pixel data values. A RWVM can be embedded within another DICOM object (such as an
408 acquired or derived image), or it can be encoded as a standalone object (National Electrical
409 Manufacturers Association (NEMA), 2016i), which in turn can either be referenced from other
410 objects, such as SRs, or recognized as being relevant from the commonality of patient and
411 study identifiers.

412 We chose to create a standalone RWVM object to encode SUVbw factor and leave the original
413 (de-identified) activity-concentration images unchanged. The RWVM object encodes the scale
414 factor, the range of stored pixel values to which it applies, and standard codes that specify the
415 quantity that the scaled (real world) value represents (in this case, the SUV), the measurement
416 method (the SUV body weight calculation method) and the measurement units (g/ml{SUVbw}).
417 The DCM coding scheme is used for the quantity and the measurement method, and, as is the
418 case throughout DICOM, the Unified Code for Units of Measure (UCUM) system (Schadow et
419 al., 1999) is used for the units. The RWVM object also includes references to all of the PET
420 image objects to which it applies.

421 The following corrections to the standard were proposed to remedy the errors or limitations of
422 the standard identified while developing DICOM representation of the SUVbw factors for this
423 project:

- 424 1. *CP 1387⁴: Addition of Quantity Descriptors to Real World Value Maps (applies to the*
425 *2014b version of the standard)* The original definition of the RWVM in DICOM only
426 defined the encoding of measurement units. We proposed an improvement to the
427 standard to include the definition of quantity in the RWVM encoding.
- 428 2. *CP 1392: Addition of Quantity Descriptors and Measurements for PET (applies to*
429 *2014b)* This CP added new concepts related to encoding of the PET measurements that
430 were missing in the standard, but were required by our use case.

431 *Image Segmentation: DICOM SEG*

432 The imaging time point was defined as an ordinal number corresponding to the imaging study
433 performed for the patient in the course of management of the specific condition, with time point

⁴ Throughout the remainder of the document we will refer to the DICOM Correction Proposals (CPs) by number; all current and past CPs are archived on the DICOM Status web page (Clunie, 2016).

434 1 corresponding to the baseline/staging study. For each such time point we encoded
435 segmentations prepared using image processing steps discussed earlier.

436 DICOM provides different mechanisms for encoding ROIs obtained by segmentation, as
437 discussed in (Fedorov et al., 2015a). The choice of the most suitable mechanism depends on
438 the use case. Since the native representation of the segmentation results were labelled
439 individual voxels, rather than a surface mesh or isocontours, we selected the DICOM
440 Segmentation image (SEG) object as the most appropriate for encoding the ROIs.

441 The SEG objects were organized as follows, to be consistent with the pattern that would likely
442 be used by tools that created them prospectively rather than retrospectively:

- 443 • Each of the RRs is stored as a separate object, since each of the RRs was segmented
444 using a distinct automatic method, using data from different modalities (the aortic arch
445 was segmented on the CT images, and the cerebellum and liver ROI were segmented
446 on the PET images).
- 447 • The primary tumor and involved lymph nodes segmented for each combination of
448 operator/segmentation method/session were stored together as different segments in a
449 single object, since both the tumor and nodes were segmented during the same session,
450 with the segmentation of one structure being identified while considering the neighboring
451 structures.
- 452 • The identifier of the operator (reader) for the manual and semi-automated segmentation
453 results was stored in the ContentCreatorName⁵ attribute.
- 454 • The identifier of the imaging time point was encoded as a positive integer, stored in the
455 ClinicalTrialTimePointID attribute.
- 456 • The identifier of the segmentation session for primary tumor and lymph nodes was
457 encoded in the ClinicalTrialSeriesID attribute.
- 458 • The type of algorithm used was encoded in the SegmentAlgorithmType attribute as
459 MANUAL, SEMIAUTOMATIC or AUTOMATIC, as appropriate.
- 460 • The suggested color for each of the segmented structures was encoded in the
461 RecommendedDisplayCIELabValue attribute.

462 The semantics of the segments were communicated using the standard AnatomicRegion (and
463 its modifier in AnatomicRegionModifier sequence, when necessary), SegmentedPropertyType
464 and SegmentedPropertyCategory sequences. For example, the semantics of a primary tumor
465 was encoded as follows:

```
466     Segmented Property Category = (M-01000, SRT, "Morphologically Altered  
467     Structure")  
468     Segmented Property Type = (M-80003, SRT, "Neoplasm, Primary")  
469     Anatomic Region = (T-53131, SRT, "base of tongue")
```

470 DICOM defines a relatively small set of segmentation property categories, listed in CID 7150
471 (National Electrical Manufacturers Association (NEMA), 2016j), and a considerably larger set of
472 segmentation property types in CID 7151 (National Electrical Manufacturers Association
473 (NEMA), 2016k). There is no direct relationship specified in the standard between category and
474 type, and the choice of an appropriate category is left to the discretion of the implementer

⁵ The CamelCase “keyword” form (without spaces) is used for clarity to identify DICOM data elements and attributes, rather than using the “name” or the parenthesized hexadecimal group and element tags.

475 (arguably the standard could be improved by grouping the types and assigning them to, and
476 requiring them for, specific categories).

477 Sometimes segmentations are performed for purely anatomical reasons (e.g., for anatomical
478 atlases), in which case there is no meaningful additional property type to record. In such cases,
479 the anatomy is encoded directly in SegmentedPropertyType, without the need for a separate
480 AnatomicRegionSequence. In other cases, segmentations are performed that apply to
481 anatomical structures, but which segment them into different types of tissue. In these cases, the
482 SegmentedPropertyType is used to encode the type of tissue (e.g., primary tumor, secondary
483 tumor, necrosis) and the AnatomicRegionSequence can be used to encode the anatomic
484 location (e.g., which organ, group of lymph nodes, etc.). Sometimes the anatomy is irrelevant
485 and not encoded at all, and the SegmentedPropertyType just encodes the type of material
486 segmented. This distinction was clarified by the authors in an earlier DICOM correction proposal
487 CP 1258. In this project we are encoding both the nature (category and type) of the segmented
488 area and its anatomic location.

489 Lymph nodes are encoded similarly, but with only the general region (head and neck) recorded
490 rather than a precise code for the lymph node group, because of the lack of the detailed
491 information about the specific lymph node name in the original dataset due to practical
492 difficulties in assigning such a precise name when segmentation was performed:

```
493     Segmented Property Category = (M-01000, SRT, "Morphologically Altered  
494     Structure")
```

```
495     Segmented Property Type = (M-80006, SRT, "Neoplasm, Secondary")  
496     Anatomic Region = (T-C4004, SRT, "lymph node of head and neck")
```

497 Semantics of the RR segmentations are communicated using the “spatial relationship concept”
498 category:

```
499     Segmented Property Category = (R-42018, SRT, "Spatial and Relational Concept")  
500     Segmented Property Type = (C94970, NCIt, "Reference Region")  
501     Anatomic Region = (T-62000, SRT, "Liver")
```

502 Binary segmentations are encoded in the PixelData attribute of the SEG object, and are
503 represented as a contiguous array of bits, with one bit per voxel for each frame. There are
504 separate frames for each slice of the volume, though all are encoded in a single multi-frame
505 object. When multiple segments (i.e., primary tumor and lymph nodes) are produced by the
506 operator during a single session using a single segmentation tool, they are stored in a single
507 SEG object, with each segment for each slice stored in a separate frame. Empty frames that do
508 not contain any voxels of the segmentation are elided, to reduce the size of the encoded
509 objects. The matrix size (rows and columns) is not abbreviated to a rectangular bounding box
510 enclosing the region of interest, which would be a further possible object size optimization (i.e.,
511 each frame has the dimensions of the original image). Similar to the RWVM objects, SEG
512 objects include references to the SOP Instance UIDs of the images (slices) that were
513 segmented.

514 The process of encoding the segmented ROIs in DICOM led to the development of the following
515 correction proposals:

- 516 1. *CP 1406: Add codes for tumor sites (applies to 2014c)* The uncoded (plain text) labels of
517 all the tumor regions used in this project were analyzed to identify common terms that
518 were then mapped to SNOMED concepts. The resulting terms were introduced into the
519 DICOM standard in the form of new context groups for lymph nodes (CID 7600) and

- 520 HNC anatomic sites (CID 7601). A distinction between concepts for primary and
521 secondary neoplasms was introduced in the same proposal.
- 522 2. *CP 1426: Correct condition in Pixel Measures, Plane Position and Orientation Functional*
523 *Groups for Segmentation (applies to 2015a)* Prior to this correction, the presence of the
524 essential attributes that are needed for volumetric reconstruction of the segmentation
525 image volumes was conditioned on attributes that were optional or not defined in
526 segmentation objects.
 - 527 3. *CP 1464: Add reference region segmentation property type (applies to 2015c)* This
528 correction added the codes needed to describe RRs, using the NCI Thesaurus
529 terminology.
 - 530 4. *CP 1496: Add Tracking Identifier and UID to Segmentation Instances (applies to 2015c)*
531 Use of a common Tracking UID allows to establish correspondence between segments
532 encoded in various segmentation objects that represent the same region being
533 segmented (i.e., across different time points, modalities, operators). Tracking UIDs were
534 already present in the SR measurements objects, which can reference segmentation
535 objects, but were not encoded directly in the segmentation objects themselves.

536 *Quantitative Measurements: DICOM SR*

537 To encode the PET SUV ROI measurements in DICOM, we specified the terminology that
538 defines the measurement quantities, modifiers and units for each measurement of interest
539 needed. The vocabulary required was not specified in any single standard context group.
540 Concepts from various standard context groups were therefore leveraged as appropriate. The
541 strategy to find a suitable term was to first consult those already in DICOM, then search for
542 related concepts in UMLS, SNOMED, and the NCI Thesaurus. If no existing concept could be
543 found, we introduced a new code and definition in a private 99PMP coding scheme, while
544 referencing a relevant publication, if available. All of the terms used are described in Appendix
545 3. The reader is referred to (Fedorov et al., 2015a) for additional discussion of the selection of
546 the quantity codes.

547 The measurements were encoded as DICOM SR objects using the standard root template TID
548 1500 defined in PS3.16 (National Electrical Manufacturers Association (NEMA), 2016l), which
549 makes use of the sub-ordinate templates shown in Fig. 4. TID 1500 contains a preamble that
550 describes general characteristics relevant to the measurement, such as an Image Library
551 container (National Electrical Manufacturers Association (NEMA), 2016m), which lists the UIDs
552 of the images in the original image series, radiopharmaceutical agent, and other items related to
553 the acquisition protocol that may be relevant during interpretation. The Imaging Measurements
554 container (section heading) includes the following attributes, which have special meaning in the
555 context of our use case:

- 556 • *Activity Session*: a positive integer that encoded the segmentation session by the
557 operator.
- 558 • *Tracking Identifier*: a human-readable identifier of the finding, which is not required to be
559 unique. In our project, RRs had tracking identifiers coded as “*referenceRegionName*
560 *reference region*”, where *referenceRegionName* was one of “liver”, “cerebellum” or
561 “aortic arch”. The primary tumor identifier was always set to “primary tumor”, individual
562 lymph nodes were identified as “lymph node *nodeID*”, where *nodeID* is a positive integer.

563 As mentioned earlier, lymph nodes were not tracked (i.e., their *nodeID* did not identify
564 the specific lymph node across time points or reading sessions).

- 565 ● *Tracking Unique Identifier*: a DICOM standard UUID-derived (random) identifier with a
566 “2.25.” prefix (National Electrical Manufacturers Association (NEMA), 2016n): a primary
567 lesion unique identifier that was used to track the lesion and reference regions across
568 time points.
- 569 ● *Time Point*: a positive integer that encoded the temporal order of the imaging study
570 within the course of management of the given patient.
- 571 ● *Referenced Segment and Source series for image segmentation*: the identifiers of the
572 segment and the segmentation object representing the ROI used in the measurement
573 group, and the identifier of the series that was segmented.
- 574 ● *Finding Site*: the coded anatomical location of the finding.

575 Related groups of measurements were encoded as a list, preceded by the codes of one or more
576 findings, following the structure defined by TID 1411 Volumetric ROI Measurements (National
577 Electrical Manufacturers Association (NEMA), 2016o), which in turn invokes TID 1419 ROI
578 Measurements (National Electrical Manufacturers Association (NEMA), 2016p), as summarized
579 in Fig. 4. Each group of measurements was derived from the ROIs that applied to the voxels of
580 a single reconstruction of a PET acquisition (image series). One SR measurement object was
581 created for each SEG object. Voxels in the ROI used for the derivation of the measurements
582 were encoded as one segment of a SEG object. Both the SEG image objects and the segment
583 number used by the derivation were referenced for each measurement group in the SR. An
584 example of the structure of the Imaging Measurements is presented in Appendix 4.

585 The following DICOM standard corrections were contributed while developing the conversion
586 methodology:

- 587 1. *CP 1366: Correction of Relationships in Planar and Volumetric ROI Templates (applies*
588 *to 2014b)* In the process of data encoding, we identified errors in the definition of the
589 relationships in some templates.
- 590 2. *CP 1386: Addition of Measurement Report Root Template for Planar and Volumetric*
591 *ROIs (applies to 2014b)* Before the introduction of this root template, measurement
592 templates could only be used to construct subordinate objects included in other
593 templates, but not to encode standalone measurement objects. This CP also added
594 some of the codes needed for this project, and allowed common content items to be
595 factored out of individual measurements to the group level.
- 596 3. *CP 1388: Add Real World Value Map Reference to Measurements (applies to 2014b)*
597 This CP added an explicit reference to the RWVM instance that was used to calculate
598 the measurements to the measurements SR object template.
- 599 4. *CP 1389: Factor Common Descriptions Out of Image Library Entries (applies to 2014b)*
600 We introduced simplifications to the structure of the measurements SR object by
601 allowing a group of images to share common image library attributes, greatly reducing
602 the size and improving the readability of the object in cases when measurements were
603 derived from many single frame images.

- 604 5. *CP 1465: Add type of finding to measurement SR templates (applies to 2015c)* The
605 measurement template was amended to include the type of finding, which is distinct from
606 its anatomical location.
- 607 6. *CP 1466: Add session to measurements group (applies to 2015c)* An extra item was
608 added to the measurement template to enable encoding of the session identifier to
609 support experiments where the measurement of the same finding is performed several
610 times in order to evaluate its repeatability.

611 Implementation of the conversion to DICOM format

612 Our overall strategy for data conversion was developed to accommodate the organization of the
613 data at the site conducting the study. Customized routines were developed to perform
614 conversion of the individual components of the data stored in the internal databases. SUV
615 normalization and quantitative measurements were calculated using the FOSS tools developed
616 as part of this project. Segmentations were converted from the results obtained before the open
617 source implementation of the semi-automatic segmentation tools was released. The top-level
618 script that was used to perform the conversion of a complete dataset by invoking conversion
619 routines for the individual data types is available in the *Iowa2DICOM* code repository (QIICR,
620 2015c).

621 *Clinical Information: DICOM SR*

622 Clinical data was exported from the internal SQL database as a tab-delimited text file. An XSLT
623 script was used to convert the tab-delimited representation into XML form, followed by another
624 XSLT transformation that produced an XML representation of an object that follows DICOM SR
625 template TID QIICR_2000 documented in Appendix 2. Finally, the resulting XML representation
626 was converted into DICOM format using existing functionality of the PixelMed toolkit (Clunie,
627 2015a). The conversion scripts are available in a public source code repository (QIICR, 2015d).
628 The DICOM series containing the clinical data DICOM SR were assigned to a study separate
629 from the one for the imaging and derived data, with both the StudyDescription and
630 SeriesDescription attribute set to "Clinical Data".

631 *Standardized Uptake Value: DICOM RWVM*

632 RWVM objects were generated in batch mode using the SUV calculation plugin of 3D Slicer
633 (QIICR, 2015e). The plugin operated on the list of files corresponding to the PET series DICOM
634 objects, calculated SUV_{bw} factor and produced a single RWVM object. Injected dose, patient
635 weight, radionuclide half-life and injection time were obtained from the DICOM PET image
636 header.

637 *Image Segmentation: DICOM SEG*

638 The process of converting segmentation results into DICOM representation was facilitated by
639 the FOSS DICOM software library implementation available in DCMTK (DICOM Toolkit) and
640 maintained by OFFIS in Germany (Eichelberg et al., 2004). To simplify the task of creating SEG
641 objects for this project and other similar efforts, we extended DCMTK with three new libraries,
642 which are now included in the official distribution of DCMTK: *dcmiod*, *dcmfg* and *dcmseg*
643 (Fedorov et al., 2015a). The conversion was performed using batch mode tools *SEG2NRRD*
644 (conversion from DICOM SEG to NRRD research format) and *EncodeSEG* (conversion from

645 research segmentation format to DICOM SEG). These tools are included in the *Iowa2DICOM*
646 repository referenced above.

647 *Volumetric Measurements: DICOM SR*

648 The process of calculation and encoding of the ROI measurements was implemented in 2 steps.
649 First, measurements of interest were calculated in batch mode using the *QuantitativeIndicesCLI*
650 tool available within PET-IndiC extension of 3D Slicer (QIICR, 2015b). The tool accepted the
651 SUV-normalized image volume and the segmentation label saved using a domain-specific
652 format, such as NRRD or NIFTI, and produced a text file encoding the measurements as key-
653 value pairs. The keys of the output correspond to the research labels assigned to the
654 measurement classes. Not all of the measurements were generated for each of the ROIs.
655 Specifically, calculation of a meaningful value for SUV peak (Wahl et al., 2009) was not possible
656 when the ROI was too small. In the cases when the measurement was not generated by the
657 tool, it was omitted from the DICOM SR measurements object.

658 Next, we used *EncodeMeasurementsSR* converter available within the *Iowa2DICOM* repository
659 (QIICR, 2015c) to generate DICOM SR objects containing the calculated measurements. This
660 converter accepted as input the list of DICOM PET object file names, the SEG object file name,
661 and the text measurements, and produced the DICOM SR object according to TID 1500. The
662 conversion utilized the *dcmsr* library of DCMTK, which provided interfaces to create and iterate
663 through a tree of DICOM SR object content.

664 *Validation of DICOM encoded objects*

665 The *dciodvfy* tool (Clunie, 2015b) was used to ensure that an object complied with the basic
666 DICOM encoding rules and contained the appropriate required attributes for the images, SEG,
667 RWVM, and SR objects. This tool did not validate compliance with specific SR templates, only
668 that valid combinations of content items and relationships were present.

669 The *dcenvfy* tool was used to validate that a set of DICOM objects contained the correct values
670 for all attributes for the same entity level in the DICOM Information Model (i.e., that all patient
671 attributes were the same for the objects with the same PatientID value, that all study attributes
672 were the same for objects with the same StudyInstanceUID value, etc.). This tool was
673 particularly helpful when objects were created along different paths or by using different tools
674 than the original images, and/or uploaded to the distribution archive on separate occasions.

675 The *com.pixelmed.validate.DicomSRValidator* tool (Clunie, 2015c) was applied to validate
676 compliance with the subset of SR templates that were supported by the tool, which included the
677 TID 1500 root template and the subordinate templates used in this project. The validation
678 consisted of checking that the required content items were present at the correct level in the
679 content tree, that conditional content items were present when specified conditions were
680 satisfied, that correct concepts and required values from specified context groups were used,
681 and that concepts were encoded with the expected code meanings. Warnings were triggered
682 when unrecognized content items were detected (which often signaled that a content item had
683 been misplaced in the tree).

684 Code availability

685 All of the code, with the exception of that for the automatic segmentation of PET RRs, is
686 available as FOSS without any restrictions on its use. Specifically, we share the following FOSS
687 tools used for PET/CT data analysis:

- 688 1. 3D Slicer (Fedorov et al., 2012) was used as the platform for implementation of all the
689 processing tools. Home page: <http://slicer.org>. Source code:
690 <http://github.org/Slicer/Slicer>.
- 691 2. PET SUV conversion: 3D Slicer *PETDICOMExtension* extension. Home page:
692 <http://wiki.slicer.org/slicerWiki/index.php/Documentation/Nightly/Modules/DICOMPETSU>
693 [VPlugin](http://wiki.slicer.org/slicerWiki/index.php/Documentation/Nightly/Modules/DICOMPETSUVPlugin). Source
694 code: [https://github.com/QIICR/Slicer-](https://github.com/QIICR/Slicer-PETDICOMExtension/tree/master/DICOMPETSUVPlugin)
[PETDICOMExtension/tree/master/DICOMPETSUVPlugin](https://github.com/QIICR/Slicer-PETDICOMExtension/tree/master/DICOMPETSUVPlugin).
- 695 3. Manual PET segmentation: Editor module of 3D Slicer (documentation and source code
696 URLs are as above for 3D Slicer).
- 697 4. Semi-automated PET segmentation: *PETTumorSegmentation* extension. Home page:
698 [http://wiki.slicer.org/slicerWiki/index.php/Documentation/4.5/Extensions/PETTumorSegm](http://wiki.slicer.org/slicerWiki/index.php/Documentation/4.5/Extensions/PETTumorSegmentation)
699 [entation](http://wiki.slicer.org/slicerWiki/index.php/Documentation/4.5/Extensions/PETTumorSegmentation). Source code: <https://github.com/QIICR/PETTumorSegmentation>.
- 700 5. PET quantitative index calculation: 3D Slicer *PET-IndiC* extension. Home page:
701 <http://wiki.slicer.org/slicerWiki/index.php/Documentation/Nightly/Extensions/PET-IndiC>.
702 Source code: <https://github.com/QIICR/PET-IndiC>.

703 In addition to the image processing tools listed above, we provide source code of the FOSS
704 tools used to create DICOM representations of the analysis results in the *Iowa2DICOM*
705 repository: <https://github.com/QIICR/Iowa2DICOM>.

706 Results

707 Clinical data and the analysis results for the total of 60 PET/CT imaging studies were encoded
708 in the DICOM format using the procedures described. One patient had a repeat imaging study.
709 The remainder had only the baseline study augmented with the clinical data and quantitative
710 analysis results DICOM objects.

711 One RWVM object, 15 SEG objects (3 RRs and tumor/lymph nodes segmentations by 3 readers
712 using 2 tools during 2 reading sessions), and 15 volumetric measurement SR objects (one per
713 SEG) were produced for each imaging study.

714 The DICOM objects were added to the QIN-HEADNECK collection of TCIA (The Cancer
715 Imaging Archive (TCIA), 2015) and are available for public access⁶. TCIA was selected for
716 archival of the resulting data since it was capable of storing and indexing the DICOM objects
717 used, and was (and still is) the QIN-recommended data sharing platform, and the analysis
718 generating the encoded data was done as part of the QIN activities at the University of Iowa.

719 Standalone validation and consistency checks were conducted as described above. In addition,
720 interoperability testing was performed as described in the remainder of this section to confirm
721 that the objects could be ingested and used by commonly available tools and toolkits: DCMTK

⁶ The SR objects encoding clinical information have restricted access due to the stipulations in the consent form under which the data was collected. Before someone can access the data they need to certify that they are using the data for research purposes and that no attempt will be made to identify the individuals. These requirements were established by the TCIA team and the Washington University IRB upon reviewing the consent forms used to collect the data.

722 (OFFIS, 2014), GDCM (Malaterre, 2015), dicom3tools (Clunie, 2009) and PixelMed (Clunie,
723 2015a).

724 The traditional DICOM encoding format is binary, and data stored in that form is most easily
725 visualized after transformation into a human-readable text format, for which different options
726 exist. One commonly used approach is to look at a so-called “dump”, which lists each attribute
727 with its tag, type (value representation), name and value (with hierarchical nesting of sequences
728 shown as required). The following publicly available tools were tested and able to successfully
729 dump the objects we created:

- 730 ● DCMTK *dcmdump* (*dump2dcm* for reverse conversion)
- 731 ● GDCM *gcmdump*
- 732 ● dicom3tools *dcdump*
- 733 ● PixelMed *com.pixelmed.dicom.AttributeList*
- 734 ● PixelMed *com.pixelmed.dicom.AttributeTreeBrowser*

735 It is also possible to convert the DICOM format into XML or JSON representations, either
736 according to schemas recently defined by the DICOM standard for this purpose (National
737 Electrical Manufacturers Association (NEMA), 2015), or using non-standard schemas. These
738 representations make the data amenable for consumption by the variety of established tools
739 such as various NoSQL databases, XML query and transformation engines, etc., and are also
740 nominally “human-readable”. We tested the following tools to confirm they could perform
741 conversion of the objects we generated into an XML representation:

- 742 ● DCMTK *dcm2xml* (*xml2dcm* for reverse conversion)
- 743 ● GDCM *gdcxml*
- 744 ● PixelMed *com.pixelmed.dicom.XMLRepresentationOfDicomObjectFactory*

745 DICOM SR objects can also be interpreted at a higher level of abstraction, which describes the
746 content items of the content tree instead of the individual attributes that compose each content
747 item. Such SR content tree “dumps” are more amenable to human interpretation than the
748 attribute level dumps. The following tools were tested to produce SR tree dumps of the objects
749 we generated:

- 750 ● DCMTK *dsrdump*
- 751 ● dicom3tools *dcsrdump*
- 752 ● PixelMed *com.pixelmed.dicom.StructuredReportBrowser*

753 DICOM SR objects can also be converted into an XML representation according to a schema
754 defined at the level of abstraction of the SR content tree rather than the individual attribute level.
755 Such representations are very suitable for integration of the DICOM data with a variety of XML-
756 oriented tools. A caveat is that DICOM has not yet established a standard schema for such a
757 conversion, so the XML representation is dependent on the schema implemented by the
758 specific tool. The following tools were tested and found to be capable of generating XML
759 representations of the DICOM SR content for the objects we generated:

- 760 ● DCMTK *dsr2xml* (*xml2dsr* for reverse conversion)
- 761 ● PixelMed *com.pixelmed.dicom.XMLRepresentationOfStructuredReportObjectFactory*
762 (bidirectional)

763 Finally, the DCMTK *dsr2html* tool can be used to generate an HTML representation of the SR
 764 content tree that can be rendered in a human-readable form in any HTML viewer. The *dsr2html*
 765 tool was tested and found to be able to render the SR objects that we generated.

766 All of the tools discussed above are command line tools. Interactive applications that wrap those
 767 command line tools are also available. The *dcmjs dump* (CommonTK, 2015) tool provides a
 768 web interface to DCMTK *dcmdump*, with the data processing done fully on the client side. The
 769 *dicom-dump* package (QIICR, 2015f) of the FOSS Atom editor wraps both *dcmdump* and
 770 *dsrdump* tools of DCMTK, and can be used to interactively invoke those tools on the DICOM
 771 objects opened in the Atom editor.

772 To illustrate the various options for examining DICOM data, we provide examples of output in
 773 different forms for the tumor measurements SR object for subject QIN-HEADNECK-01-00024.
 774 At the level of DICOM attributes, measurement of the SUVbw peak is shown in Fig. 5. Another
 775 view of this same portion of the object in DCMTK-specific SR XML is shown in Fig. 6.

776 By comparison, an SR tree level text dump of the same content as produced by *dsrdump*
 777 appears as follows:

```
778 <contains NUM:(126401,DCM,"SUVbw") =
779     "5.90721" ({SUVbw}g/ml,UCUM,"Standardized Uptake Value body weight")>
780     <has concept mod CODE:(121401,DCM,"Derivation") = (126031,DCM,"Peak Value
781     Within ROI")>
```

782 A rendered view of a section of the HTML representation of the same object as produced by
 783 *dsr2html* is shown in Fig. 7.

784 The foregoing checks did not serve to test more complex application-level interoperability.
 785 Additional tests were performed for the SEG objects. Since ROIs encoded as segmentations
 786 may be visualized in relation to the images from which they were segmented, we investigated
 787 the interoperability of several imaging workstations with respect to their ability to correctly render
 788 segmentations superimposed on the PET images. The following software was tested:

- 789 • 3D Slicer (*Reporting* extension, starting from Nov 22, 2015 nightly build version)
- 790 • ePAD v1.7 (Stanford Medicine, 2015)
- 791 • AIM on ClearCanvas v4.6.0.3 (Mongkolwat, 2015)
- 792 • Brainlab PDM v2.2 (commercial workstation) (Brainlab AG, Feldkirchen, Germany)

793 Each of these platforms was capable of successfully importing the SEG objects and displaying
 794 the encoded segments. An example of the rendering of the segmentations in 3D Slicer is shown
 795 in Fig. 8.

796 Discussion

797 Realistic quantitative imaging research scenarios necessitate the use of a variety of data
 798 sources and processing routines, making the results of such analyses inherently complex. Our
 799 goal was to provide a complete and reproducible description of the process, both from the data
 800 modeling and implementation perspectives. A key strategy for mitigation of complexity is the
 801 provision of appropriate tools. We hope that the burden of complexity on the individual
 802 researcher can be minimized, whilst reusability and interoperability can be maximized, by
 803 leveraging and improving existing DICOM FOSS tools and toolkits, instrumenting widely used

804 research applications with DICOM capability, and providing a clear path selecting and linking an
805 appropriate, relevant, and sufficient subset of DICOM capabilities for the research use case.

806 We believe this work is the first to demonstrate the utility of the DICOM standard for
807 interoperable quantitative result encoding in the QI research domain, complete with the publicly
808 available FOSS implementing the conversion and interpretation/visualization tools, encoded
809 objects and documentation describing the specialized templates used for data encoding.
810 Furthermore, we intentionally described the details of the various correction proposals that were
811 contributed to the standard in the course of our work, to demonstrate that DICOM is an evolving
812 standard that is open to improvements as needed to support research use cases. The
813 improvements to the standard contributed by this project have wider applicability and, we hope,
814 will greatly simplify the task for adopters of the DICOM approach.

815 The tools available in the *Iowa2DICOM* repository were developed for the specific HNC QI use
816 case presented in this manuscript. As such, the repository has served the intended purpose of
817 producing the dataset described, and is not maintained. We provide the source code of
818 *Iowa2DICOM* to facilitate reproducible research and to provide technical insight into our
819 methods. The SEG converters can be used for general purposes and have since been
820 incorporated in 3D Slicer to enable import and export of DICOM SEG objects. We are also
821 working on the next iteration of the conversion tools in the new *dcmqi* (DICOM for QI) library
822 (QIICR, 2016) to provide general purpose DICOM conversion tools. Unlike *Iowa2DICOM*, which
823 is dependent on 3D Slicer build tree, *dcmqi* is self-contained. It is under development and will be
824 maintained by the QIICR project. As of writing, *dcmqi* incorporates the SEG conversion tools
825 and includes basic examples, sample datasets and usage instructions.

826 Data conversion, as implemented and described in this paper, was performed retrospectively.
827 We did not use DICOM as the operational data format, but instead adopted it to enable archival
828 and sharing of the final analysis results, since the purpose was to reuse data already acquired
829 for a research study to test the hypothesis, rather than wait until improved tools were fully
830 deployed for prospective data acquisition. We are not arguing that retrospective conversion is
831 preferred, quite the contrary. It is practical though, since historical analysis pipelines often
832 contain tools developed using different toolkits and languages that may not yet have support for
833 the various DICOM objects we utilized. The installed base of research tools may also not yet
834 contain sufficient mechanisms for maintaining and propagating the patient and study level
835 information (the composite context). Our project demonstrates how, in situations like the one
836 encountered in this project, composite context can be recovered and merged into the shared
837 results retrospectively, to re-associate acquired images, derived results and clinical data.
838 Addressing this key barrier to interoperability with the clinical environment should be a high
839 priority for the research community, particularly since scalability to large experiments and the
840 conduct of clinical trials (especially those spread across multiple sites or using multiple tools),
841 requires a solution to manage data identity and provenance. That said, the choice of format for
842 interoperable exchange versus that for internal operational use can remain distinct to the extent
843 deemed appropriate for any particular research scenario.

844 The work presented in this paper is a step towards improving support of quantitative imaging
845 research use cases in DICOM, and improving support of the relevant parts of the DICOM
846 standard in both FOSS and commercial tools and toolkits. We are actively engaged in improved
847 integration of DCMTK with 3D Slicer to provide streamlined user interfaces that empower end

848 users to store the results of their work as appropriate DICOM objects with minimum extra effort.
849 Although the specific use case described in this paper involve PET/CT, the approach has broad
850 applicability for interoperable communication of segmentation and quantitative analysis results
851 independent of the imaging modality. At the level of developer toolkits, we have recently
852 completed the implementation of an API in DCMTK to support abstractions related to the
853 generation of volumetric measurement SR objects (TID 1500)⁷. We are also in the process of
854 extending the DCMTK API to support the creation of Enhanced Multi-frame objects for Magnetic
855 Resonance Imaging (MRI). We are planning to use that functionality for other QI biomarker use
856 cases being investigated by QIICR that focus on the use of multiparametric MRI in glioblastoma
857 and prostate cancer. To support those use cases that involve analyses that generate derived
858 functional maps of tissue properties, QIICR has also contributed to the development of the
859 Parametric Map object in DICOM (National Electrical Manufacturers Association (NEMA),
860 2016q), now part of the standard, which supports encoding of floating point pixel data without
861 being restricted to rescaling of integer values, finally resolving a longstanding perceived
862 weakness of DICOM for research applications.

863 Another area of QIICR focus is the development of tools to ease the process of interacting with
864 the standard and exploring the content of DICOM data. In this area, we have developed an
865 initial version of a DICOM search index that provides fast an alternative interface to explore the
866 DICOM standard (QIICR, 2015g), and contributed the *dicom-dump* package to the popular Atom
867 editor discussed earlier (QIICR, 2015f). These additional activities are intended to assist a
868 diverse variety of groups, which include academic QI researchers (both technical and clinical),
869 software developers implementing QI analysis tools, clinical end users, and developers of the
870 commercial tools deploying QI biomarkers. Our goal is to make it easier for interested parties to
871 explore, evaluate and implement DICOM capabilities relevant for QI research. We hope these
872 efforts will contribute to the technical solution of the overarching problem of standardized and
873 meaningful sharing of reproducible research results, as well as improve the integration of the
874 research tools with clinical systems to facilitate the translation of QI biomarker clinical trials and
875 clinical research studies into clinical practice.

876 Conclusions

877 We have presented a detailed investigation of the development and application of the DICOM
878 standard and supporting FOSS tools to encode research data for quantitative imaging
879 biomarker development. Using the real-life research scenario of HNC PET/CT quantitative
880 image analysis, we demonstrated that the DICOM standard is capable of representing various
881 types of analysis results and their interrelationships. The resulting data objects are annotated in
882 a standard manner, and utilize consistent and widely used codes for communicating semantics.
883 They are also interoperable with the variety of tools readily available to the researcher, as well
884 as commercial clinical imaging and analysis systems (which universally support many aspects
885 of the DICOM standard).

⁷ The API abstractions to support generation of DICOM SR documents following TID 1500 were completed after the data conversion described in this manuscript was finished. Therefore, the SR converter from the *Iowa2DICOM* repository referenced in the text utilizes a lower level API, which could be greatly simplified with the recent improvements to the DCMTK *dcmsr* module. These improvements will be implemented in the new *dcmqi* library.

886 The work presented is a result of two years of activities of the QIICR project, but it builds upon
887 the foundation established by the various research groups, communities and FOSS projects,
888 such as 3D Slicer and DCMTK, decades before QIICR. We are committed to continue working
889 with those groups and communities, as well as other stakeholders and adopters interested in
890 remedying the *status quo* of very limited sharing of the quantitative image analysis results in the
891 imaging community.

892 Acknowledgments

893 We thank John Sunderland for the help with PET/CT image acquisition; Markus van Tol for his
894 contribution to the implementation of the PET tumor segmentation module in 3D Slicer; Kirk
895 Smith for his help in archiving the DICOM data on TCIA; Jean-Christophe Fillion-Robin, Andras
896 Lasso, Nicole Aucoin, Christian Herz, and the 3D Slicer community for their contribution to the
897 development of the relevant 3D Slicer functionality.

898 Evaluation of interoperability of the resulting DICOM segmentation objects with ePAD, AIM on
899 ClearCanvas and Brainlab tools was performed as part of a Quantitative Imaging Reading
900 Room exhibit at the 2015 convention of the Radiological Society of North America (RSNA)
901 (Fedorov et al., 2015b). We thank Daniel Rubin, Pattanasak Mongkolwat and David Flade for
902 providing access to and facilitating testing of the interoperability of the respective tools.

903 References

- 904 Bauer C., Sun S., Sun W., Otis J., Wallace A., Smith BJ., Sunderland JJ., Graham MM., Sonka
905 M., Buatti JM., Beichel RR. 2012. Automated measurement of uptake in cerebellum, liver,
906 and aortic arch in full-body FDG PET/CT scans. *Medical physics* 39:3112–3123. DOI:
907 10.1118/1.4711815.
- 908 Bidgood WD Jr. 1997. Documenting the information content of images. *Proceedings: a
909 conference of the American Medical Informatics Association / ... AMIA Annual Fall
910 Symposium. AMIA Fall Symposium:424–428.*
- 911 Bidgood WD Jr., Korman LY., Golichowski AM., Hildebrand PL., Mori AR., Bray B., Brown NJG.,
912 Spackman KA., Dove SB., Schoeffler K. 1997. Controlled terminology for clinically-relevant
913 indexing and selective retrieval of biomedical images. *International Journal on Digital
914 Libraries* 1:278–287.
- 915 Bidgood WD Jr. 1998. The SNOMED DICOM microglossary: controlled terminology resource for
916 data interchange in biomedical imaging. *Methods of information in medicine* 37:404–414.
- 917 Bodenreider O. 2004. The Unified Medical Language System (UMLS): integrating biomedical
918 terminology. *Nucleic acids research* 32:D267–70. DOI: 10.1093/nar/gkh061.
- 919 Boellaard R. 2009. Standards for PET image acquisition and quantitative data analysis. *Journal
920 of nuclear medicine: official publication, Society of Nuclear Medicine* 50 Suppl 1:11S–20S.
921 DOI: 10.2967/jnumed.108.057182.
- 922 Boulton G., Rawlins M., Vallance P., Walport M. 2011. Science as a public enterprise: the case
923 for open data. *The Lancet* 377:1633–1635. DOI: 10.1016/S0140-6736(11)60647-8.
- 924 Chan A-W., Song F., Vickers A., Jefferson T., Dickersin K., Gøtzsche PC., Krumholz HM.,
925 Gherzi D., van der Worp HB. 2014. Increasing value and reducing waste: addressing
926 inaccessible research. *The Lancet* 383:257–266. DOI: 10.1016/S0140-6736(13)62296-5.
- 927 Clark K., Vendt B., Smith K., Freymann J., Kirby J., Koppel P., Moore S., Phillips S., Maffitt D.,
928 Pringle M., Tarbox L., Prior F. 2013. The Cancer Imaging Archive (TCIA): Maintaining and
929 Operating a Public Information Repository. *Journal of digital imaging*. DOI:
930 10.1007/s10278-013-9622-7.

- 931 Clunie D. 2000. *DICOM Structured Reporting*. PixelMed Publishing.
- 932 Clunie D. 2009. Dicom3tools Software. Available at <http://www.dclunie.com/dicom3tools.html>
933 (accessed November 22, 2015).
- 934 Clunie D. 2015a. PixelMed Java DICOM Toolkit. Available at
935 <http://pixelmed.com/#PixelMedJavaDICOMToolkit> (accessed November 22, 2015).
- 936 Clunie D. 2015b. DICOM Validator - dciodvfy. Available at
937 <http://www.dclunie.com/dicom3tools/dciodvfy.html> (accessed November 22, 2015).
- 938 Clunie D. 2015c. DicomSRValidator. Available at
939 [http://www.dclunie.com/pixelmed/software/javadoc/com/pixelmed/validate/DicomSRValidat
940 or.html](http://www.dclunie.com/pixelmed/software/javadoc/com/pixelmed/validate/DicomSRValidator.html) (accessed November 22, 2015).
- 941 Clunie D. 2016. DICOM Standard Status. Available at [http://www.dclunie.com/dicom-
942 status/status.html](http://www.dclunie.com/dicom-status/status.html) (accessed February 17, 2016).
- 943 CommonTK. 2015. dcmjs by commontk. Available at <http://dcmjs.org/dump/index.html>
944 (accessed November 19, 2015).
- 945 Cornet R., de Keizer N. 2008. Forty years of SNOMED: a literature review. *BMC medical
946 informatics and decision making* 8 Suppl 1:S2. DOI: 10.1186/1472-6947-8-S1-S2.
- 947 Eichelberg M., Riesmeier J., Wilkens T., Hewett AJ., Barth A., Jensch P. 2004. Ten years of
948 medical imaging standardization and prototypical implementation: the DICOM standard and
949 the OFFIS DICOM toolkit (DCMTK). In: *Medical Imaging 2004*. International Society for
950 Optics and Photonics, 57–68. DOI: 10.1117/12.534853.
- 951 Fedorov A., Beichel R., Kalpathy-Cramer J., Finet J., Fillion-Robin J-CC., Pujol S., Bauer C.,
952 Jennings D., Fennessy F., Sonka M., Buatti J., Aylward S., Miller J V., Pieper S., Kikinis R.
953 2012. 3D Slicer as an image computing platform for the Quantitative Imaging Network.
954 *Magnetic resonance imaging* 30:1323–1341. DOI: 10.1016/j.mri.2012.05.001.
- 955 Fedorov A., Clunie D., Ulrich E., Bauer C., Wahle A., Brown B., Onken M., Riesmeier J., Pieper
956 S., Kikinis R., Buatti J., Beichel RR. 2015a. DICOM for quantitative imaging biomarker
957 development: A standards based approach to sharing of clinical data and structured
958 PET/CT analysis results in head and neck cancer research. *PeerJ PrePrints*. DOI:
959 10.7287/peerj.preprints.1541v3.
- 960 Fedorov A., Rubin D., Kalpathy-Cramer J., Kirby J., Clunie D., Onken M., Flade F., Mongkolwat
961 P., Venkateraman R., Bertling J., Pieper S., Kikinis R. 2015b. Interoperable communication
962 of quantitative image analysis results using DICOM standard.
- 963 Graham MM., Peterson LM., Hayward RM. 2000. Comparison of simplified quantitative
964 analyses of FDG uptake. *Nuclear medicine and biology* 27:647–655.
- 965 Haak D., Page CE., Kabino K., Deserno TM. 2015. Evaluation of DICOM viewer software for
966 workflow integration in clinical trials. In: *SPIE Medical Imaging*. International Society for
967 Optics and Photonics, 94180O–94180O–9. DOI: 10.1117/12.2082051.
- 968 Ibanez L., Schroeder WJ. 2005. *The ITK Software Guide 2.4*. Kitware, Inc.
- 969 Interoperability Working Group (AFUL). 2015. Definition of Interoperability. Available at
970 <http://interoperability-definition.info/en/> (accessed November 11, 2015).
- 971 Katzan IL., Rudick RA. 2012. Time to integrate clinical and research informatics. *Science
972 translational medicine* 4:162fs41. DOI: 10.1126/scitranslmed.3004583.
- 973 Kindlmann G. 2004. Teem: NRRD - Nearly Raw Raster Data. Available at
974 <http://teem.sourceforge.net/nrrd/> (accessed November 16, 2015).
- 975 Krishnaraj A., Weinreb JC., Ellenbogen PH., Allen B Jr., Norbash A., Kazerooni EA. 2014. The
976 Future of Imaging Biomarkers in Radiologic Practice: Proceedings of the Thirteenth Annual
977 ACR Forum. *Journal of the American College of Radiology: JACR* 11:20–23. DOI:
978 10.1016/j.jacr.2013.08.017.
- 979 Larson SM., Erdi Y., Akhurst T., Mazumdar M., Macapinlac HA., Finn RD., Casilla C., Fazzari
980 M., Srivastava N., Yeung HWD., Humm JL., Guillem J., Downey R., Karpeh M., Cohen AE.,
981 Ginsberg R. 1999. Tumor Treatment Response Based on Visual and Quantitative Changes

- 982 in Global Tumor Glycolysis Using PET-FDG Imaging. The Visual Response Score and the
983 Change in Total Lesion Glycolysis. *Clinical positron imaging: official journal of the Institute*
984 *for Clinical P.E.T* 2:159–171.
- 985 Lucignani G., Paganelli G., Bombardieri E. 2004. The use of standardized uptake values for
986 assessing FDG uptake with PET in oncology: a clinical perspective. *Nuclear medicine*
987 *communications* 25:651–656.
- 988 Malaterre M. 2015. Grassroots DICOM (GDCM). Available at
989 <http://sourceforge.net/projects/gdcm/> (accessed November 19, 2015).
- 990 Marcus D., Olsen T., Ramaratnam M., Buckner R. 2007. The Extensible Neuroimaging Archive
991 Toolkit: an informatics platform for managing, exploring, and sharing neuroimaging data.
992 *Neuroinformatics* 5:11–33. DOI: 10.1385/NI:5:1:11.
- 993 McDonald CJ., Vreeman DJ., Abhyankar S. 2013. Comment on “time to integrate clinical and
994 research informatics.” *Science translational medicine* 5:179le1. DOI:
995 10.1126/scitranslmed.3005700.
- 996 Mongkolwat P. 2015. AIM on ClearCanvas. Available at
997 <http://www.ict.mahidol.ac.th/research/Imaging-Informatics> (accessed November 29, 2015).
- 998 Moore SM., Maffitt DR., Smith KE., Kirby JS., Clark KW., Freymann JB., Vendt BA., Tarbox LR.,
999 Prior FW. 2015. De-identification of Medical Images with Retention of Scientific Research
1000 Value. *Radiographics: a review publication of the Radiological Society of North America,*
1001 *Inc* 35:727–735. DOI: 10.1148/rg.2015140244.
- 1002 MRC Cognition and Brain Sciences Unit. 2013. The Analyze Data Format. Available at
1003 <http://imaging.mrc-cbu.cam.ac.uk/imaging/FormatAnalyze> (accessed November 16, 2015).
- 1004 National Electrical Manufacturers Association (NEMA). 2015. A Data Exchange Models. In:
1005 *DICOM PS3.19 2015c - Application Hosting*.
- 1006 National Electrical Manufacturers Association (NEMA). 2016a. D DICOM Controlled
1007 Terminology Definitions (Normative). In: *DICOM PS3.16 - Content Mapping Resource*.
- 1008 National Electrical Manufacturers Association (NEMA). 2016b. A.21 Positron Emission
1009 Tomography Image IOD. In: *DICOM PS3.3 - Information Object Definitions*.
- 1010 National Electrical Manufacturers Association (NEMA). 2016c. A.3 Computed Tomography
1011 Image IOD. In: *DICOM PS3.3 - Information Object Definitions*.
- 1012 National Electrical Manufacturers Association (NEMA). 2016d. E.2 Basic Application Level
1013 Confidentiality Profile. In: *DICOM PS3.15 - Security and System Management Profiles*.
- 1014 National Electrical Manufacturers Association (NEMA). 2016e. A.35.3 Comprehensive SR IOD.
1015 In: *DICOM PS3.3 - Information Object Definitions*.
- 1016 National Electrical Manufacturers Association (NEMA). 2016f. *DICOM PS3.16 - Content*
1017 *Mapping Resource*.
- 1018 National Electrical Manufacturers Association (NEMA). 2016g. TID 3802 Cardiovascular Patient
1019 History. In: *DICOM PS3.16 - Content Mapping Resource*.
- 1020 National Electrical Manufacturers Association (NEMA). 2016h. Relevant Patient Information
1021 Templates. In: *DICOM PS3.16 - Content Mapping Resource*.
- 1022 National Electrical Manufacturers Association (NEMA). 2016i. A.46 Real World Value Mapping
1023 IOD. In: *DICOM PS3.3 - Information Object Definitions*.
- 1024 National Electrical Manufacturers Association (NEMA). 2016j. CID 7150 Segmentation Property
1025 Categories. In: *DICOM PS3.16 - Content Mapping Resource*.
- 1026 National Electrical Manufacturers Association (NEMA). 2016k. CID 7151 Segmentation Property
1027 Types. In: *DICOM PS3.16 - Content Mapping Resource*.
- 1028 National Electrical Manufacturers Association (NEMA). 2016l. TID 1500 Measurement Report.
1029 In: *DICOM PS3.16 - Content Mapping Resource*.
- 1030 National Electrical Manufacturers Association (NEMA). 2016m. TID 1600 Image Library. In:
1031 *DICOM PS3.16 - Content Mapping Resource*.
- 1032 National Electrical Manufacturers Association (NEMA). 2016n. B.2 UUID Derived UID. In:

- 1033 *DICOM PS3.5 - Data Structures and Encoding.*
1034 National Electrical Manufacturers Association (NEMA). 2016o. TID 1411 Volumetric ROI
1035 Measurements. In: *DICOM PS3.16 - Content Mapping Resource.*
1036 National Electrical Manufacturers Association (NEMA). 2016p. TID 1419 ROI Measurements. In:
1037 *DICOM PS3.16 - Content Mapping Resource.*
1038 National Electrical Manufacturers Association (NEMA). 2016q. A.75 Parametric Map IOD. In:
1039 *DICOM PS3.3 - Information Object Definitions.*
1040 National Electrical Manufacturers Association (NEMA). DICOM Homepage. Available at
1041 <http://dicom.nema.org/> (accessed November 11, 2015).
1042 NIFTI Data Format Working Group. 2005.NIFTI: — Neuroimaging Informatics Technology
1043 Initiative. Available at <http://nifti.nimh.nih.gov/> (accessed November 16, 2015).
1044 OFFIS. 2014. DCMTK - DICOM Toolkit. Available at <http://dicom.offis.de/dcmTk> (accessed
1045 December 29, 2015).
1046 Piwowar HA., Vision TJ. 2013. Data reuse and the open data citation advantage. *PeerJ* 1:e175.
1047 DOI: 10.7717/peerj.175.
1048 QIICR. 2015a. QIICR/PETTumorSegmentation. Available at
1049 <https://github.com/QIICR/PETTumorSegmentation> (accessed November 23, 2015).
1050 QIICR. 2015b. QIICR/PET-IndiC. Available at <https://github.com/QIICR/PET-IndiC> (accessed
1051 November 22, 2015).
1052 QIICR. 2015c. QIICR/Iowa2DICOM. Available at <https://github.com/QIICR/Iowa2DICOM>
1053 (accessed November 22, 2015).
1054 QIICR. 2015d. QIICR/IowaHNClinicalDataDICOMSRConversion. Available at
1055 <https://github.com/QIICR/IowaHNClinicalDataDICOMSRConversion> (accessed November
1056 22, 2015).
1057 QIICR. 2015e. QIICR/Slicer-PETDICOMExtension. Available at [https://github.com/QIICR/Slicer-](https://github.com/QIICR/Slicer-PETDICOMExtension)
1058 *PETDICOMExtension* (accessed November 22, 2015).
1059 QIICR. 2015f. dicom-dump: DICOM viewer for Atom. Available at
1060 <https://atom.io/packages/dicom-dump> (accessed November 19, 2015).
1061 QIICR. 2015g. A Searchable Index of the DICOM Base Standard 2015c. Available at
1062 https://fedorov.cloudant.com/dicom_search/.site/index.html (accessed November 19, 2015).
1063 QIICR. 2016. dcmqi. Available at <https://github.com/QIICR/dcmqi> (accessed March 23, 2016).
1064 Schadow G., McDonald CJ., Suico JG., Föhring U., Tolxdorff T. 1999. Units of measure in
1065 clinical information systems. *Journal of the American Medical Informatics Association:*
1066 *JAMIA* 6:151–162.
1067 Schroeder WJ., Martin KM. 2005. The Visualization Toolkit. In: *Visualization Handbook.*
1068 Elsevier, 593–LV. DOI: 10.1016/B978-012387582-2/50032-0.
1069 Semantic Web - W3C 2015. Available at <http://www.w3.org/standards/semanticweb/> (accessed
1070 November 17, 2015).
1071 Stanford Medicine. 2015. ePAD | web-based platform for quantitative imaging in the clinical
1072 workflow. Available at <https://epad.stanford.edu/> (accessed November 24, 2015).
1073 Stodden VC. 2010. Reproducible Research: Addressing the Need for Data and Code Sharing in
1074 Computational Science. *Computing in science & engineering* 12:8–13. DOI:
1075 10.1109/MCSE.2010.113.
1076 The Cancer Imaging Archive (TCIA). 2015. QIN-HEADNECK - The Cancer Imaging Archive
1077 (TCIA) Public Access - Cancer Imaging Archive Wiki. Available at
1078 <https://wiki.cancerimagingarchive.net/display/Public/QIN-HEADNECK> (accessed November
1079 19, 2015).
1080 Vanderhoek M., Perlman SB., Jeraj R. 2012. Impact of the definition of peak standardized
1081 uptake value on quantification of treatment response. *Journal of nuclear medicine: official*
1082 *publication, Society of Nuclear Medicine* 53:4–11. DOI: 10.2967/jnumed.111.093443.
1083 Van Tol M., Ulrich EJ., Bauer C., Chang T., Plichta KA., Smith BJ., Sunderland JJ., Graham

- 1084 MM., Sonka M., Buatti JM., Beichel RR. 2016. Semi-automated Segmentation of Head and
1085 Neck Cancers in 18F-FDG PET Scans: A Just-Enough-Interaction Approach. *Medical*
1086 *physics*.
- 1087 Wahl RL., Jacene H., Kasamon Y., Lodge MA. 2009. From RECIST to PERCIST: Evolving
1088 Considerations for PET response criteria in solid tumors. *Journal of nuclear medicine:*
1089 *official publication, Society of Nuclear Medicine* 50 Suppl 1:122S–50S. DOI:
1090 10.2967/jnumed.108.057307.
- 1091 Walport M., Brest P. 2011. Sharing research data to improve public health. *The Lancet*
1092 377:537–539. DOI: 10.1016/S0140-6736(10)62234-9.
- 1093 Waterton JC., Pylkkanen L. 2012. Qualification of imaging biomarkers for oncology drug
1094 development. *European journal of cancer* 48:409–415. DOI: 10.1016/j.ejca.2011.11.037.
- 1095 Weber WA. 2006. Positron emission tomography as an imaging biomarker. *Journal of clinical*
1096 *oncology: official journal of the American Society of Clinical Oncology* 24:3282–3292. DOI:
1097 10.1200/JCO.2006.06.6068.
- 1098 Yin Y., Zhang X., Williams R., Wu X., Anderson DD., Sonka M. 2010. LOGISMOS -- Layered
1099 Optimal Graph Image Segmentation of Multiple Objects and Surfaces: Cartilage
1100 Segmentation in the Knee Joint. *IEEE transactions on medical imaging* 29:2023–2037.
1101 DOI: 10.1109/TMI.2010.2058861.

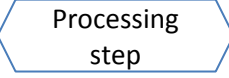
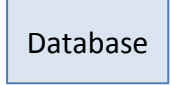
1102

Figure 1(on next page)

Diagram of the interaction among the various data sources and processing steps that result in the dataset described in this paper.

Components of the dataset represented in DICOM are released publicly within the TCIA QIN-HEADNECK collection. FOSS tools corresponding to the processing steps other than Reference Region (RR) segmentation (processing steps with the dashed outline) are available.

Legend

-  Data represented in the DICOM format
-  Data represented in a research format
-  Processing step
-  Database

Segmentations marked with * may contain more than one structure segmented

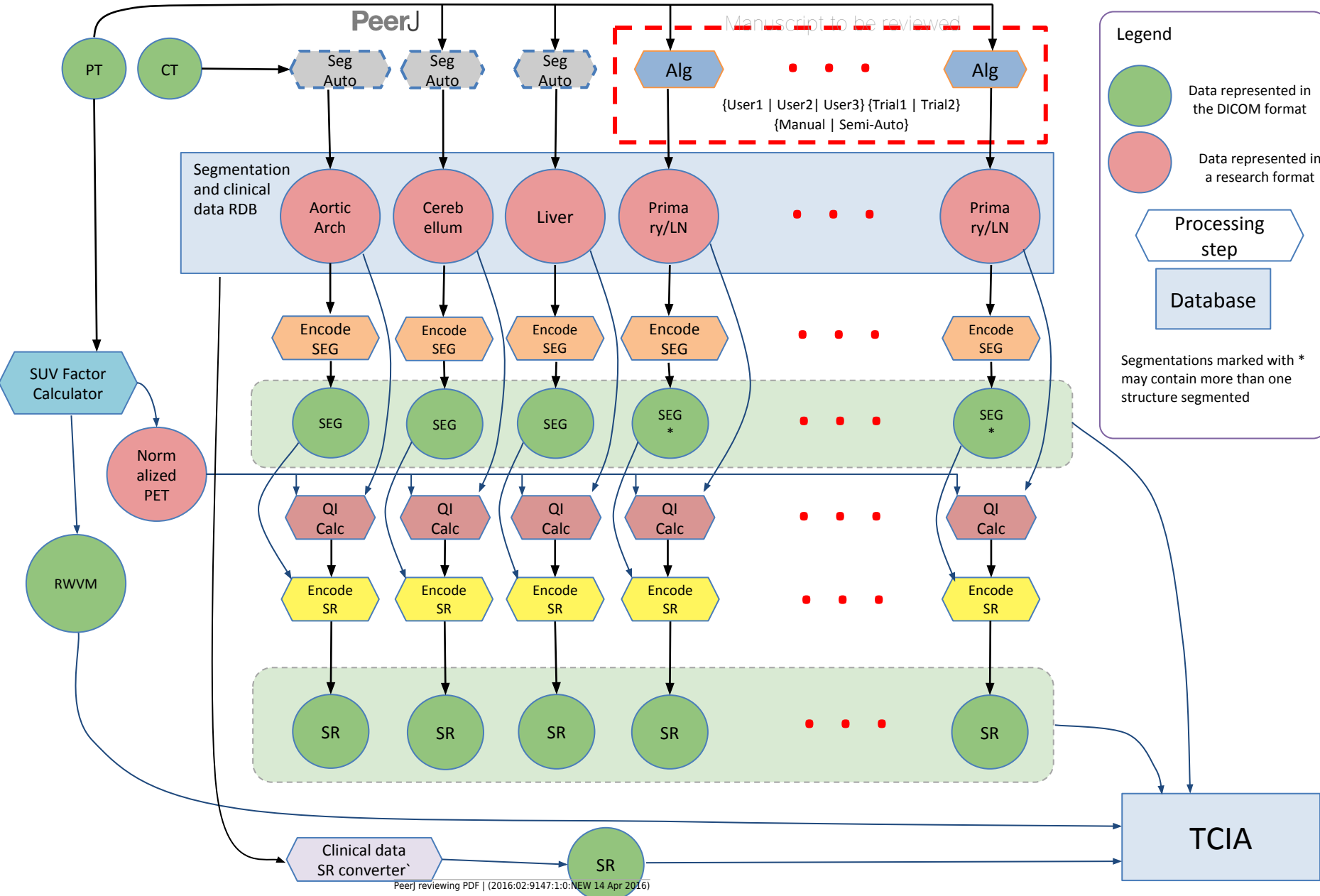


Figure 2(on next page)

An illustration of the relationships among the DICOM objects discussed in this manuscript.

DICOM PET/CT is the original dataset obtained by the imaging equipment and is modified only by the de-identification procedure. DICOM RWVM, SEG, and measurement SR are derived objects. DICOM SR with the clinical information encodes the information about the patient originally stored in the relational database. Solid lines denote explicit reference of the object instances by the derived objects (referenced instance is pointed to by the arrow). Dashed bidirectional arrows denote commonality of identifiers (i.e., common composite context, e.g., at the Patient and Study level).

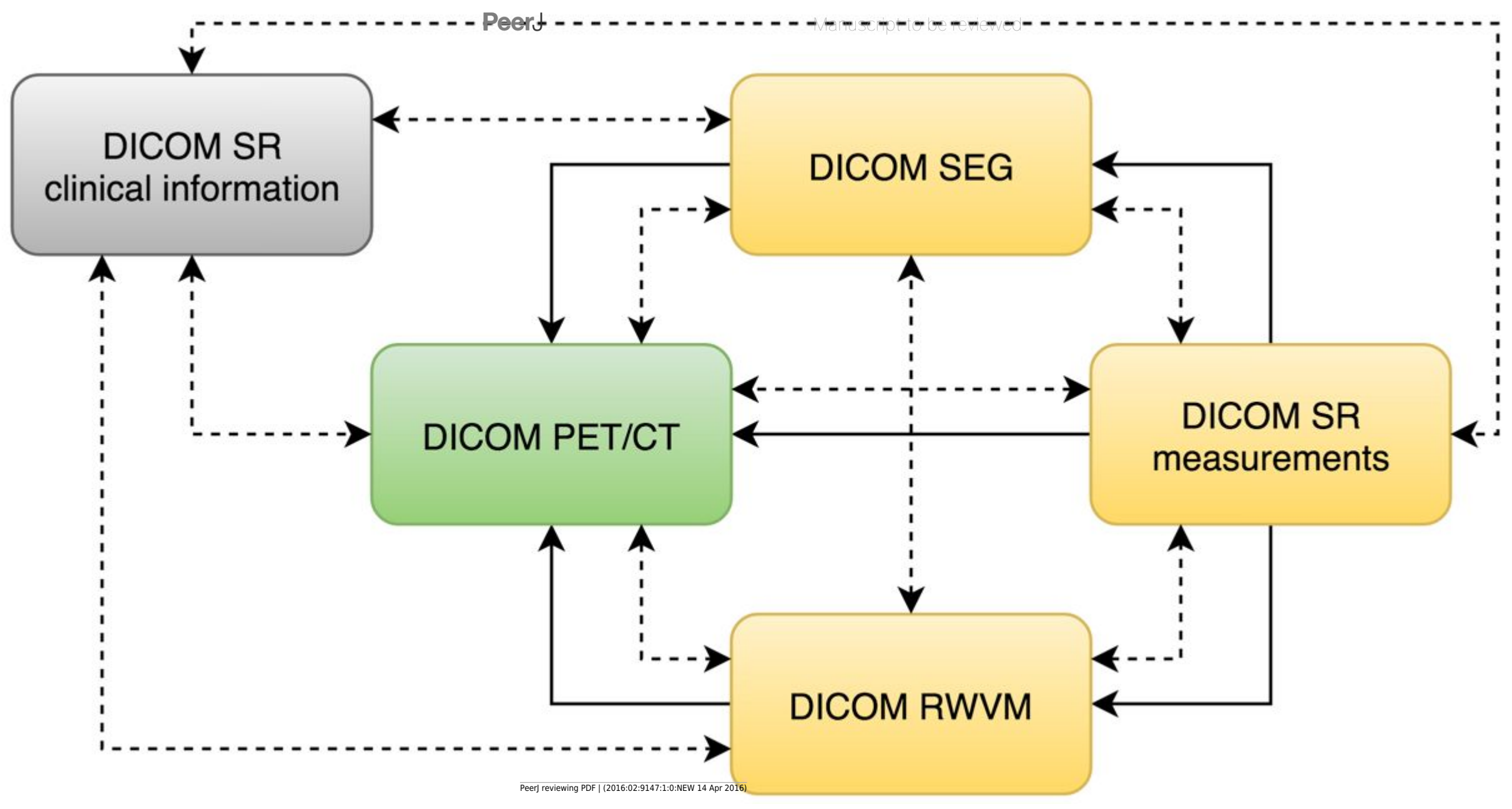


Figure 3(on next page)

Relationships of the private DICOM SR templates used for encoding of the clinical information.

The top-level Clinical Data Report template incorporates subordinate templates, described in detail in Appendix 2.

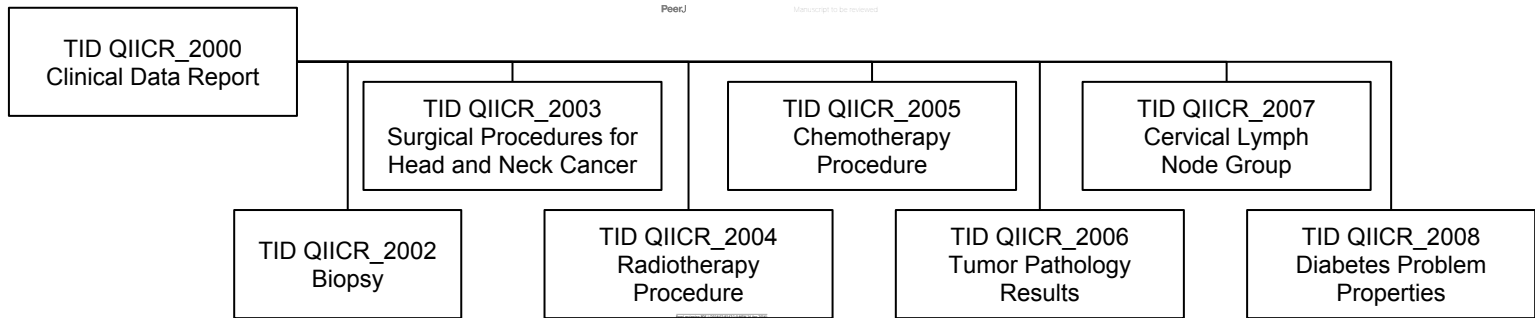


Figure 4(on next page)

The family of DICOM SR templates used for communicating the PET measurements.

All of the templates used to encode derived measurements are included in the DICOM standard.

TID 1500
Imaging Measurement
Report

TID 1204
Language of Content
Items and Descendants

TID 1411
Volumetric ROI
Measurements

TID 1001
Observation
Context

TID 1600
Image Library

TID 1502
Time Point Context

TID 1419
ROI Measurements

5

An attribute-level dump corresponding to the section of the DICOM SR measurements.

The text shown is an excerpt of the complete object dump encoding SUVbw peak value for subject QIN-HEADNECK-01-0024, series “tumor measurements - User1 Manual trial 1”, as displayed in the Atom editor using dicom-dump package.

**Note: Auto Gamma Correction was used for the image. This only affects the reviewing manuscript. See original source image if needed for review.*

```

5757 ..... (ffff,e000) na (Item with undefined length #=5) # u/l, 1 Item
5758 ..... (0040,a010) CS [CONTAINS] # 8, 1 RelationshipType
5759 ..... (0040,a040) CS [NUM] # 4, 1 ValueType
5760 ..... (0040,a043) SQ (Sequence with undefined length #=1) # u/l, 1 ConceptNameCodeSequence
5761 ..... (ffff,e000) na (Item with undefined length #=3) # u/l, 1 Item
5762 ..... (0008,0100) SH [126401] # 6, 1 CodeValue
5763 ..... (0008,0102) SH [DCM] # 4, 1 CodingSchemeDesignator
5764 ..... (0008,0104) LO [SUVbw] # 6, 1 CodeMeaning
5765 ..... (ffff,e00d) na (ItemDelimitationItem) # 0, 0 ItemDelimitationItem
5766 ..... (ffff,e0dd) na (SequenceDelimitationItem) # 0, 0 SequenceDelimitationItem
5767 ..... (0040,a300) SQ (Sequence with undefined length #=1) # u/l, 1 MeasuredValueSequence
5768 ..... (ffff,e000) na (Item with undefined length #=2) # u/l, 1 Item
5769 ..... (0040,00ea) SQ (Sequence with undefined length #=1) # u/l, 1 MeasurementUnitsCodeSequence
5770 ..... (ffff,e000) na (Item with undefined length #=3) # u/l, 1 Item
5771 ..... (0008,0100) SH [(SUVbw)g/mL] # 12, 1 CodeValue
5772 ..... (0008,0102) SH [UCUM] # 4, 1 CodingSchemeDesignator
5773 ..... (0008,0104) LO [Standardized Uptake Value body weight] # 38, 1 CodeMeaning
5774 ..... (ffff,e00d) na (ItemDelimitationItem) # 0, 0 ItemDelimitationItem
5775 ..... (ffff,e0dd) na (SequenceDelimitationItem) # 0, 0 SequenceDelimitationItem
5776 ..... (0040,a30a) DS [5.90721] # 8, 1 NumericValue
5777 ..... (ffff,e00d) na (ItemDelimitationItem) # 0, 0 ItemDelimitationItem
5778 ..... (ffff,e0dd) na (SequenceDelimitationItem) # 0, 0 SequenceDelimitationItem
5779 ..... (0040,a730) SQ (Sequence with undefined length #=1) # u/l, 1 ContentSequence
5780 ..... (ffff,e000) na (Item with undefined length #=4) # u/l, 1 Item
5781 ..... (0040,a010) CS [HAS CONCEPT MOD] # 16, 1 RelationshipType
5782 ..... (0040,a040) CS [CODE] # 4, 1 ValueType
5783 ..... (0040,a043) SQ (Sequence with undefined length #=1) # u/l, 1 ConceptNameCodeSequence
5784 ..... (ffff,e000) na (Item with undefined length #=3) # u/l, 1 Item
5785 ..... (0008,0100) SH [121401] # 6, 1 CodeValue
5786 ..... (0008,0102) SH [DCM] # 4, 1 CodingSchemeDesignator
5787 ..... (0008,0104) LO [Derivation] # 10, 1 CodeMeaning
5788 ..... (ffff,e00d) na (ItemDelimitationItem) # 0, 0 ItemDelimitationItem
5789 ..... (ffff,e0dd) na (SequenceDelimitationItem) # 0, 0 SequenceDelimitationItem
5790 ..... (0040,a168) SQ (Sequence with undefined length #=1) # u/l, 1 ConceptCodeSequence
5791 ..... (ffff,e000) na (Item with undefined length #=3) # u/l, 1 Item
5792 ..... (0008,0100) SH [126031] # 6, 1 CodeValue
5793 ..... (0008,0102) SH [DCM] # 4, 1 CodingSchemeDesignator
5794 ..... (0008,0104) LO [Peak Value Within ROI] # 22, 1 CodeMeaning
5795 ..... (ffff,e00d) na (ItemDelimitationItem) # 0, 0 ItemDelimitationItem
5796 ..... (ffff,e0dd) na (SequenceDelimitationItem) # 0, 0 SequenceDelimitationItem
5797 ..... (ffff,e00d) na (ItemDelimitationItem) # 0, 0 ItemDelimitationItem
5798 ..... (ffff,e0dd) na (SequenceDelimitationItem) # 0, 0 SequenceDelimitationItem
5799 ..... (ffff,e00d) na (ItemDelimitationItem) # 0, 0 ItemDelimitationItem

```

6

An XML representation corresponding to the section of the DICOM SR measurements.

The excerpt shown is encoding SUVbw peak measurement for subject QIN-HEADNECK-01-0024, series "tumor measurements - User1 Manual trial 1".

**Note: Auto Gamma Correction was used for the image. This only affects the reviewing manuscript. See original source image if needed for review.*

```
4530 ..... <num>.....
4531 ..... <relationship>CONTAINS</relationship>.....
4532 ..... <concept>.....
4533 ..... <value>126401</value>.....
4534 ..... <scheme>.....
4535 ..... <designator>DCM</designator>.....
4536 ..... </scheme>.....
4537 ..... <meaning>SUVbw</meaning>.....
4538 ..... </concept>.....
4539 ..... <code>.....
4540 ..... <relationship>HAS_CONCEPT_MOD</relationship>.....
4541 ..... <concept>.....
4542 ..... <value>121401</value>.....
4543 ..... <scheme>.....
4544 ..... <designator>DCM</designator>.....
4545 ..... </scheme>.....
4546 ..... <meaning>Derivation</meaning>.....
4547 ..... </concept>.....
4548 ..... <value>126031</value>.....
4549 ..... <scheme>.....
4550 ..... <designator>DCM</designator>.....
4551 ..... </scheme>.....
4552 ..... <meaning>Peak Value Within ROI</meaning>.....
4553 ..... </code>.....
4554 ..... <value>5.90721</value>.....
4555 ..... <unit>.....
4556 ..... <value>{SUVbw}g/ml</value>.....
4557 ..... <scheme>.....
4558 ..... <designator>UCUM</designator>.....
4559 ..... </scheme>.....
4560 ..... <meaning>Standardized Uptake Value body weight</meaning>.....
4561 ..... </unit>.....
4562 ..... </num>.....
```

7

A rendered view of an HTML representation of the SR measurements object tree.

The content shown is for subject QIN-HEADNECK-01-0024, series “tumor measurements - User1 Manual trial 1”, as generated by the DCMTK dsr2html tool and rendered in a Chrome browser. SUVbw peak measurement is highlighted by the red rectangle.

Measurement Group

Observation Context: Activity Session = "1"
Observation Context: Tracking Identifier = "lymph node 1"
Observation Context: Tracking Unique Identifier = 2.25.322107966936615591151071083168045938604

Finding:

Neoplasm, Secondary (M-80006, SRT)

Observation Context: Time Point = "1"

Referenced Segment:

[SG image](#)

Source series for image segmentation:

1.3.6.1.4.1.14519.5.2.1.2744.7002.117357550898198415937979788256

Real World Value Map used for measurement:

[RealWorldValueMappingStorage](#)

Concept Modifier: Measurement Method = SUV body weight calculation method (126410, DCM)
Concept Modifier: Finding Site = lymph node of head and neck (T-C4004, SRT)

SUVbw:

3.71385 {SUVbw}g/ml

Concept Modifier: Derivation = Mean (R-00317, SRT)

SUVbw:

1.67934 {SUVbw}g/ml

Concept Modifier: Derivation = Minimum (R-404FB, SRT)

SUVbw:

7.20806 {SUVbw}g/ml

Concept Modifier: Derivation = Maximum (G-A437, SRT)

SUVbw:

5.90721 {SUVbw}g/ml

Concept Modifier: Derivation = Peak Value Within ROI (126031, DCM)

Volume:

8.95531 ml

Concept Modifier: Measurement Method = Sum of segmented voxel volumes (126030, DCM)

Total Lesion Glycolysis:

33.2587 g

SUVbw:

1.14615 {SUVbw}g/ml

Concept Modifier: Derivation = Standard Deviation (R-10047, SRT)

SUVbw:

2.84535 {SUVbw}g/ml

Concept Modifier: Derivation = 25th Percentile Value (250137, 99PMP)

8

Example of the segmentation results visualization initialized from DICOM representation.

Shown is subject QIN-HEADNECK-01-00024, as displayed in 3D Slicer software. The primary tumor (AnatomicRegionSequence = (T-53131,SRT,"base of tongue"), SegmentedPropertyCategory = (M-01000,SRT,"Morphologically Altered Structure"), SegmentedPropertyType = (M-80003,SRT,"Neoplasm, Primary")) is shown in green and the lymph node metastasis (AnatomicRegionSequence = (T-C4004,SRT,"lymph node of head and neck"), SegmentedPropertyCategory = (M-01000,SRT,"Morphologically Altered Structure"), SegmentedPropertyType = (M-80006,SRT,"Neoplasm, Secondary")) in yellow. Small window on the foreground demonstrates communication of the segmented regions semantics. Panel on the left shows axial cross-section of the PET image volume, with the segmentation outline in the overlay. On the right is volume rendered portion of the image composed with the axial cross-section and surface rendering of the secondary tumor.

